TECTONICS, VOL. 26, TC5015, doi:10.1029/2007TC002128, 2007

Detrital zircon age and Hf isotopic studies for metasedimentary rocks from the Chinese Altai: Implications for the Early Paleozoic tectonic evolution of the Central Asian Orogenic Belt

Xiaoping Long,[1,2] Min Sun,[2] Chao Yuan,[1] Wenjiao Xiao,[3] Shoufa Lin,[4] Fuyuan Wu,[3] Xiaoping Xia,[2] and Keda Cai[1]

Received 7 March 2007; revised 29 June 2007; accepted 19 July 2007; published 16 October 2007.

[1] The Chinese Altai, a typical region of the Central Asian Orogenic Belt (CAOB), has been envisaged as subduction-accretion complex or Precambrian microcontinent. Thick metasedimentary rocks crop out extensively in the Central Altai and Qiongkuer domains, but their depositional age is not well constrained. Most workers have regarded these sedimentary rocks as passive continental margin sediments deposited on a Precambrian microcontinent. However, our studies of U-Pb and Hf isotopes of detrital zircons separated from these rocks reveal that a predominant population has $^{206}Pb/^{238}U$ ages between 460 and 540 Ma and most grains of this population possess positive $\varepsilon_{Hf}(t)$ values. Zircons of the population have oscillatory zoning, possess high Th/U ratios, and are enhedral to subhedral crystals with sharp edges, showing short distance of transportation from an igneous provenance. The above results indicate that these metasedimentary rocks were deposited on an active continental margin not prior to the Middle Ordovician. Therefore the Chinese Altai orogen was an active continental margin in the Early Paleozoic, which is inconsistent with a Precambrian microcontinent model and reveals an arc accretionary history. **Citation:** Long, X., M. Sun, C. Yuan, W. Xiao, S. Lin, F. Wu, X. Xia, and K. Cai (2007), Detrital zircon age and Hf isotopic studies for metasedimentary rocks from the Chinese Altai: Implications for the Early Paleozoic tectonic evolution of the Central Asian Orogenic Belt, *Tectonics*, *26*, TC5015, doi:10.1029/2007TC002128.

1. Introduction

[2] The Central Asian Orogenic Belt (also named Altaids or Altaid collage) is the largest Phanerozoic orogenic belt in the world, extending from the Urals in the west to the Pacific Ocean in the east and from Siberia in the north to the Tianshan in the south. During the closure of the Paleo-Asian Ocean, a large number of allochthonous terranes including island arcs, submarine plateaus/seamounts, and possibly some microcontinental blocks were accreted in this orogen [e.g., *Sengör et al.*, 1993; *Dobretsov et al.*, 1995; *Sengör and Natal'in*, 1996; *Jahn et al.*, 2000; *Jahn*, 2004; *Windley et al.*, 2002; *Badarch et al.*, 2002; *Khain et al.*, 2003; *Dobretsov et al.*, 2004; *Hong et al.*, 2004; *Kuzmichev et al.*, 2005; *Helo et al.*, 2006]. However, the allochthonous natures of these terranes, the variety of their original tectonic environments and the different amalgamation times, have made it difficult to unravel the geological evolution of the Central Asian Orogenic Belt. For example, the Chinese segment of this orogen (the Chinese Altai) has been envisaged as a Paleozoic fold belt [*Li et al.*, 1982; *Ren et al.*, 1999], passive continental margin [*He et al.*, 1990], subduction-accretion complex [*Sengör and Natal'in*, 1996], or a Precambrian microcontinent [e.g., *Li et al.*, 2006]. In order to determine the accretionary history of this region, these tectonic models must be vigorously tested.

[3] The Chinese Altai is mainly made up of six fault-bound NW–SE extending allochthonous terranes [e.g., *He et al.*, 1990; *Windley et al.*, 2002; *Xiao et al.*, 2004]. The Central Altai and Qiongkuer are two largest tectonic domains forming the backbone of this orogen (Figure 1). The Central Altai Domain (Terranes 2 and 3 of *Windley et al.* [2002]) consists of gneissic rocks, metasedimentary rocks and granitic plutons. The high-grade metamorphic rocks have commonly been considered to be the Proterozoic basement of the orogen [e.g., *Li et al.*, 1996]. The metasedimentary rocks include a very thick (7754 m [*Bureau of Geology Mineral Resources of Xinjiang Uygur Autonomous Region* (*BGMRX*), 1993]) slate-phyllite-schist sequence named Habahe Group. The protoliths of these rocks were fine-grained sandstone, siltstone and mudstone with flysch rhythm. Their age of deposition is not very well constrained, and they have been assigned variably to the Middle-Upper Ordovician [*Group for Compilation of Regional Stratigraphy of Xinjiang* (*GCRSX*), 1981], Sinian [*Wang*, 1983; *Peng*, 1989] or Sinian-Cambrian [*BGMRX*, 1993]. This sedimentary sequence is generally regarded as a passive continental

[1]Key Laboratory of Isotope Geochronology and Geochemistry, Guangzhou Institute of Geochemistry, Chinese Academy of Sciences, Guangzhou, China.
[2]Department of Earth Sciences, University of Hong Kong, Hong Kong, China.
[3]State Key Laboratory of Lithospheric Evolution, Institute of Geology and Geophysics, Chinese Academy of Sciences, Beijing, China.
[4]Department of Earth Sciences, University of Waterloo, Waterloo, Ontario, Canada.

0278-7407/07/2007TC002128$12.00

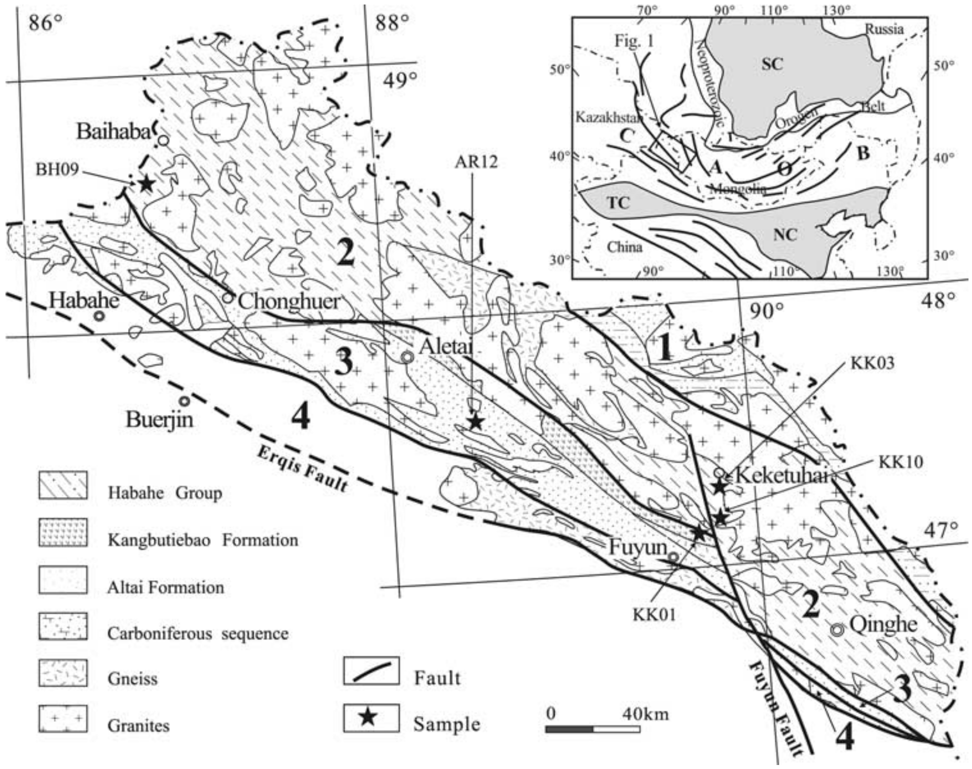

Figure 1. Simplified geological map of the Chinese Altai orogen, modified from *He et al.* [1990] and *Windley et al.* [2002]. Domains: 1, North Altai; 2, Central Altai; 3, Qiongkuer; 4, Erqis. The inset shows a simplified tectonic map of the Central Asian Orogen Belt. Abbreviation: SC, Siberian Craton; NC, North China Craton; TC, Tarim Craton; CAOB, Central Asian Orogenic Belt.

margin deposit [e.g., *Li et al.*, 2006]. To the southwest, this domain is separated by a series of thrusts from the Qiongkuer Domain (Terranes 4 of *Windley et al.* [2002]), which are mainly composed of turbiditic and volcanic rocks and divided into the Kangbutiebao and Altai Formations. The two formations were assigned to upper Silurian to lower Devonian and Middle Devonian respectively [e.g., *BGMRX*, 1993; *Windley et al.*, 2002; *Li et al.*, 2003], and considered to deposit in rift-related environment of a passive continental margin [e.g., *Li et al.*, 2006].

[4] Because detrital zircons can survive erosion, transportation, diagenesis, metamorphism and even crustal partial melting, U-Pb geochronology of detrital zircons is a very powerful tool for sedimentary provenance studies [*McLennan et al.*, 2001; *Guan et al.*, 2002; *Fedo et al.*, 2003; *Andersen et al.*, 2004; *Payne et al.*, 2006; *Moecher and Samson*, 2006; *Luo et al.*, 2004; *Xia et al.*, 2006a]. In order to avoid bias in grain selection and obtain reliable results, an adequate number of zircon grains must be analyzed [*Fedo et al.*, 2003]. Hf isotopic compositions of detrital zircons can also help in tracing the nature of their provenance [e.g., *Griffin et al.*, 2004; *Xia et al.*, 2006b]. In the current study, metasedimentary samples from the Central Altai and Qiongkuer domains were collected for U-Pb dating and Hf isotopic studies of detrital zircons. Our data place firm constraints on the age and nature of the source provenance of these metasediments, which shed light on the tectonic evolutionary history of the Chinese Altai.

2. Regional Geological Setting

[5] The Altai orogen is situated between the Sayan and associated belts to the north and the Junggar basin to the south, extending for several thousand kilometers from Russia, Kazakhstan, through North Xinjiang, to South Mongolia [*Coleman*, 1989; *Xiao et al.*, 1992; *Zorin et al.*, 1993; *Zhang et al.*, 1993; *Federovskii et al.*, 1995]. The Chinese segment of this orogen consists of six fault-bound NW–SE extending allochthonous terranes [e.g., *He et al.*, 1990; *Windley et al.*, 2002; *Xiao et al.*, 2004]. Each of these terranes have distinctive stratigraphy, metamorphism and deformation pattern, and was developed in different times. The Central Altai Domain is the largest domain and contains gneissic rocks, metasedimentary rocks and granitic plutons (Figure 1). The gneissic rocks were previously considered to be high-degree metamorphic rocks of the Habahe Group, but were later assigned to the Paleo- to Meso-proterozoic Kemuqi and Neoproterozoic Fuyun Groups [e.g., *Li et al.*, 1996; *Chen et al.*, 2003] and hence were considered to be Proterozoic basement of the Chinese Altai [e.g., *He et al.*, 1990; *Windley et al.*, 2002; *Li et al.*, 2006]. This interpretation is based mainly on Sm-Nd

isotopic data for the high-grade metamorphic rocks [*D. H. Wang et al.*, 2002; *Hu et al.*, 2002], Nd model age [e.g., *Hu et al.*, 2000] and zircon xenocryst age [e.g., *Windley et al.*, 2002] for the granitoids intruding these metamorphic rocks.

[6] The Habahe Group (or called the Hanasi Group [*BGMRX*, 1993]) crops out widely in the Central Altai Domain, which was previously divided into the Central Altaishan and NW Altaishan terranes [*Windley et al.*, 2002; *Li et al.*, 2003; *Yuan et al.*, 2007] (Figure 1). This group consists largely of quartzo-feldspathic clastic turbidites [*He et al.*, 1990; *Li et al.*, 2006], which have been isoclinally folded with steep axial planes and metamorphosed under low greenschist facies conditions [*Windley et al.*, 2002]. In the field, these rocks occur as slate-phyllite-schist, derived from the original fine-grained sandstone, siltstone, and mudstone. This group was originally assigned a Middle to Late Ordovician age, but recent workers favored a Sinian or Sinian to Middle Ordovician age [e.g., *GCRSX*, 1981; *Wang*, 1983; *Peng*, 1989; *BGMRX*, 1993; *Windley et al.*, 2002; *Chen and Jahn*, 2002; *Li et al.*, 2006], and suggested that it was deposited in a passive continental margin of a Precambrian continent block [e.g., *He et al.*, 1990; *Li and Poliyangsiji*, 2001; *Li et al.*, 2006].

[7] In the southwest, the Central Altai Domain is in fault contact with the Qiongkuer Domain (Figure 1), which is made up of the Kangbutiebao and Altai Formations and locally metamorphosed to gneisses or schists [e.g., *Li et al.*, 2003]. The Kangbutiebao Formation is 1–2 km thick and consists of upper Silurian to lower Devonian volcanic and pyroclastic rocks, with minor basic volcanic rocks and spilites [*Han and He*, 1991; *Windley et al.*, 2002]. Resting on this unit is the Middle Devonian Altai Formation, which consists mainly of a turbiditic sandstone-siltstone-mudstone sequence, with minor pillow-bearing basalts and siliceous volcanics, representing a deep-water flysch sequence [*Li et al.*, 2003]. Rocks of this domain were previously considered to have formed in a rifting tectonic setting [e.g., *He et al.*, 1990; *Han and He*, 1991; *Li*, 1991], but more recently have been assigned to arc and fore-arc environments [*Windley et al.*, 2002].

3. Sample Description

[8] Sample KK03 is a mica schist from the Habahe Group, collected 5 km south of Keketuohai (N47°10′52.7″ E89°46′48.7″). The sample is grey in color and composed mainly of quartz (45–65 modal%), plagioclase (15–25 modal%), biotite (10–25 modal%) and minor chlorite (<5 modal%). The rock is strongly foliated, with biotite and chlorite showing open-folded schistosity.

[9] Sample KK10 is a migmatized metasedimentay rock from the Habahe Group, collected about 20 km south of Keketuohai (N47°06′40.9″ E89°49′25.3″). Leucosomes composed of medium-grained quartz (30–40 modal%), plagioclase (20–25 modal%), orthoclase (20–30 modal%) and biotite (10–15 modal%) form 0.5- to 2-cm-thick bands. The melanosomes form 0.3- to 1.2-cm-thick bands and consist of biotite (40–50 modal%), chlorite (5–10 modal%), plagioclase (10–15 modal%), orthoclase (10–20 modal%) and quartz (<10 modal%), with minor magnetite, apatite and zircon.

[10] Sample BH09 is a siltstone from the Habahe Group, collected about 25 km southwest of Baihaba (N48°32′19.6″ E86°42′17.2″). The siltstone is well sorted, slightly metamorphosed and weakly deformed. The sample consists of rounded clasts of quartz and plagioclase (60–80 modal%) in a fine-grained matrix of quartz and lithic fragments (20–35 modal%).

[11] Sample KK01 is a mylonite from the Kangbutiebao Formation, collected 30 km east of Fuyun (N46°59′48.7″ E89°44′41.6″). The mylonites in this area, which occur along the Fuyun Fault, consist mainly of quartz (75–85 modal%), plagioclase (~15 modal%) and biotite (~5 modal%), with minor amounts of muscovite and ilmenite. Some rounded and deformed grains of quartz and plagioclase form porphyroclasts in a matrix composed of fine-grained recrystallized quartz. Recrystallized biotite occurs as very fine-grained aggregates showing foliation.

[12] Sample AR12 is a garnet-sillimanite gneiss from the Altai Formation, collected 50 km southeast of Aletai city (N47°34′53.7″ E88°25′11.3″). The rock consists of medium- to fine-grained quartz (55–65 modal%), plagioclase (15–20 modal%), biotite (10–15 modal%), garnet (<5 modal%) and sillimanite (<5 modal%), with minor amounts of magnetite. The garnet forms subhedral, pink-colored grains, whereas the sillimanite is acicular and the biotite occurs as dark flakes that define the gneissosity. The mineral assemblage and high percentages of Al-rich minerals imply that this sample is a paragneiss.

4. Analytical Method

4.1. Zircon Separation and CL Imaging

[13] Zircon is a common accessory mineral in the samples collected, and was separated by using heavy liquid and magnetic techniques. Zircon grains from the >25 μm nonmagnetic fractions were hand-picked. About 100 grains were randomly selected and mounted on adhesive tape, then enclosed in epoxy resin and polished to about half of their diameter. After being photographed under reflected and transmitted light, the samples were prepared for Cathodoluminescence (CL) imaging, U-Pb dating and Hf isotope analysis.

[14] In order to investigate the origin and structure of zircons and to choose target sites for U-Pb and Hf isotopic analyses, CL imaging was carried out using a JXA-8100 Electron Probe Microanalyzer with Mono CL3 Cathodoluminescence System for high-resolution imaging and spectroscopy at the Guangzhou Institute of Geochemistry, Chinese Academy of Sciences.

4.2. U-Pb Isotope Analysis

[15] All zircon grains of each sample in the mount were analyzed. Their U-Pb isotopic compositions were analyzed on a VG PQ Excel ICP-MS equipped with New Wave Research LUV213 laser ablation system, installed in the Department of Earth Sciences, the University of Hong Kong. The laser system delivers a beam of 213 nm UV

light from a frequency-quintupled Nd: YAG laser. Most analyses were carried out with a beam diameter of 40 μm, 10 Hz repetition rate, and energy of 0.6–1.3 mJ per pulse. This gave ^{238}U signal of 3×10^4 to 200×10^4 counts per second, depending on U contents. Typical ablation time was 30–60 s, resulting in pits 20–40 μm deep. The instrumental settings and detailed analytical procedures have been described by *Xia et al.* [2004]. U–Pb ages of zircons were calculated using the U decay constants of ^{238}U = 1.55125×10^{-10} year^{-1}, ^{235}U = 9.8454×10^{-10} year^{-1} and the Isoplot 3 software [*Ludwig*, 2003]. Individual analyses are presented with 1σ error in Table A1 in Appendix A and in concordia diagrams, and uncertainties in age results are quoted at 95% level (1σ). In this study, ^{207}Pb/^{206}Pb ages are used for zircons older than 1000 Ma, but ^{206}Pb/^{238}U ages are used for zircons younger than 1000 Ma, because the relative small amount of ^{207}Pb accumulated in young zircons does not permit precise ^{207}Pb/^{206}Pb dating. The error correlation of ^{206}Pb/^{238}U – ^{207}Pb/^{235}U used in the Concordia plot is 0.85, a value from a long-term statistics of the laboratory.

4.3. Hf Isotope Analysis

[16] Hf isotope analysis was carried out using an ArF excimer laser ablation system, attached to a Neptune Plasma multicollector ICP-MS, at the Institute of Geology and Geophysics, Chinese Academy of Science in Beijing. The analyses for zircon grains from the mica schist and garnet-sillimanite gneiss were conducted with a beam diameter of 32 μm, 8 Hz repetition rate, and energy of 15 mJ/cm^2, whereas a beam diameter of 63 μm and 6 Hz repetition rate were used for the other samples. Both settings yielded a signal intensity of $\sim$10 V at ^{180}Hf for the standard zircon 91500. Typical ablation time was 26 s, resulting in pits 20–30 μm deep. Masses 172, 173, 175–180 and 182 were simultaneously measured in static-collection mode. Data were normalized to ^{176}Hf/^{177}Hf = 0.7325, using exponential correction for mass bias. Owing to the extremely low ^{176}Lu/^{177}Hf in zircon (normally <0.002), the isobaric interference of ^{176}Lu on ^{176}Hf is negligible [*Iizuka and Hirata*, 2005]. The mean β_{Yb} value was applied for the isobaric interference correction of ^{176}Yb on ^{176}Hf in the same spot. The ratio of ^{176}Yb/^{172}Yb (0.5887) is also applied for the Yb correction. Detailed instrumental settings and analytical procedures are described by *Wu et al.* [2006]. The measured ^{176}Lu/^{177}Hf ratios and the ^{176}Lu decay constant of 1.865×10^{-11} yr^{-1} reported by *Scherer et al.* [2001] were used to calculate initial ^{176}Hf/^{177}Hf ratios. The chondritic values of ^{176}Hf/^{177}Hf = 0.0332 and ^{176}Lu/^{177}Hf = 0.282772 reported by *Blichert-Toft and Albarede* [1997] were used for the calculation of ε_{Hf}(t) values. The depleted mantle line is defined by present-day ^{176}Hf/^{177}Hf = 0.28325 and ^{176}Lu/^{177}Hf = 0.0384 [*Griffin et al.*, 2004]. Because zircons are generally formed in granitic magma derived from the lower crust, the two-style model ages (T^c_{DM}) are more meaningful than the depleted mantle model ages. The mean ^{176}Lu/^{177}Hf ratio of 0.008 for the upper continental crust [*Taylor and McLennan*, 1985] was used to calculate T^c_{DM} and the following discussion in this study is based on the T^c_{DM} ages.

5. Results

[17] The U-Pb ages and Hf isotope compositions are given in Tables A1 and A2, respectively. Because detrital zircon grains in any given sample may have been derived from different sources, all zircon grains from each sample in the mount were analyzed for U-Pb isotope compositions. The Hf isotopic analyses were preformed on the same selected zircon domains of U-Pb dating.

[18] The CL images show that most detrital zircons from our samples are enhedral to subhedral crystals with sharp edges, and have concentric oscillatory zoning (Figure 2). These features, along with their high Th/U ratios (>0.1, Table A1), indicate that the zircons had an igneous provenances. A few detrital zircons are low luminescent and nebulously zoned (Figure 2), but their high Th/U ratios also suggest an igneous origin [*Hanchar and Rundnick*, 1995]. Some detrital zircons from the garnet-sillimanite gneiss (Sample AR12) have low luminescent rims with low Th/U ratios (<0.1, Table A1) and lack oscillatory zoning. These rims are interpreted as metamorphic overgrowths [e.g., *Hoskin and Black*, 2000; *Corfu et al.*, 2003].

5.1. Schist From the Habahe Group (Sample KK03)

[19] Fifty-eight detrital zircons from this sample were analyzed successfully for U-Pb isotopic compositions. These zircon grains form two distinct groups (Figure 2): one group consists of enhedral to subhedral grains with concentric oscillatory zoning and sharp edge ($\sim$64%), whereas the other consists of rounded anhedral, homogeneous grains or ones with nebulous zoning ($\sim$36%). Most of the analyses from this sample are concordant or nearly concordant (Table A1). About eighty percent of the first type gave ^{206}Pb/^{238}U ages between 468 Ma and 541 Ma, and other twenty percent yielded 547 Ma to 586 Ma ^{206}Pb/^{238}U ages (Table A1). Of the second type (rounded zircons), eight gave ^{206}Pb/^{238}U ages between 721 Ma and 932 Ma, and additional eight yielded Paleoproterozoic ^{207}Pb/^{206}Pb ages (1722–2284 Ma) (Table A1 and Figure 3). We notice that one zircon has an early formed zircon core (Figure 2), which yielded a ^{207}Pb/^{206}Pb age of 2411 Ma. A similar ^{207}Pb/^{206}Pb age (2453 Ma) was also obtained from another rounded zircon. A discordant analytical point yielded an older ^{207}Pb/^{206}Pb age of 2721 Ma (Figure 3). Moreover, a concordant detrital zircon with Archean ^{207}Pb/^{206}Pb age of 3087 ± 20 Ma was first discovered, which confirmed Archean material in the source. In the Gaussian probability diagram, a 515 Ma peak is prominent for zircons from this sample (Figure 4).

[20] Twenty-two detrital zircons from this sample were also analyzed for Hf isotopic compositions (Table A2). The ε_{Hf}(t) values vary widely from –20 to +14 (Figure 5), which indicates a complex provenance for the zircons. The Hf model ages for these detrital zircons are mainly Mesoproterozoic to Neoproterozoic, with only four data points falling in the Archean (3.0–3.3 Ga).

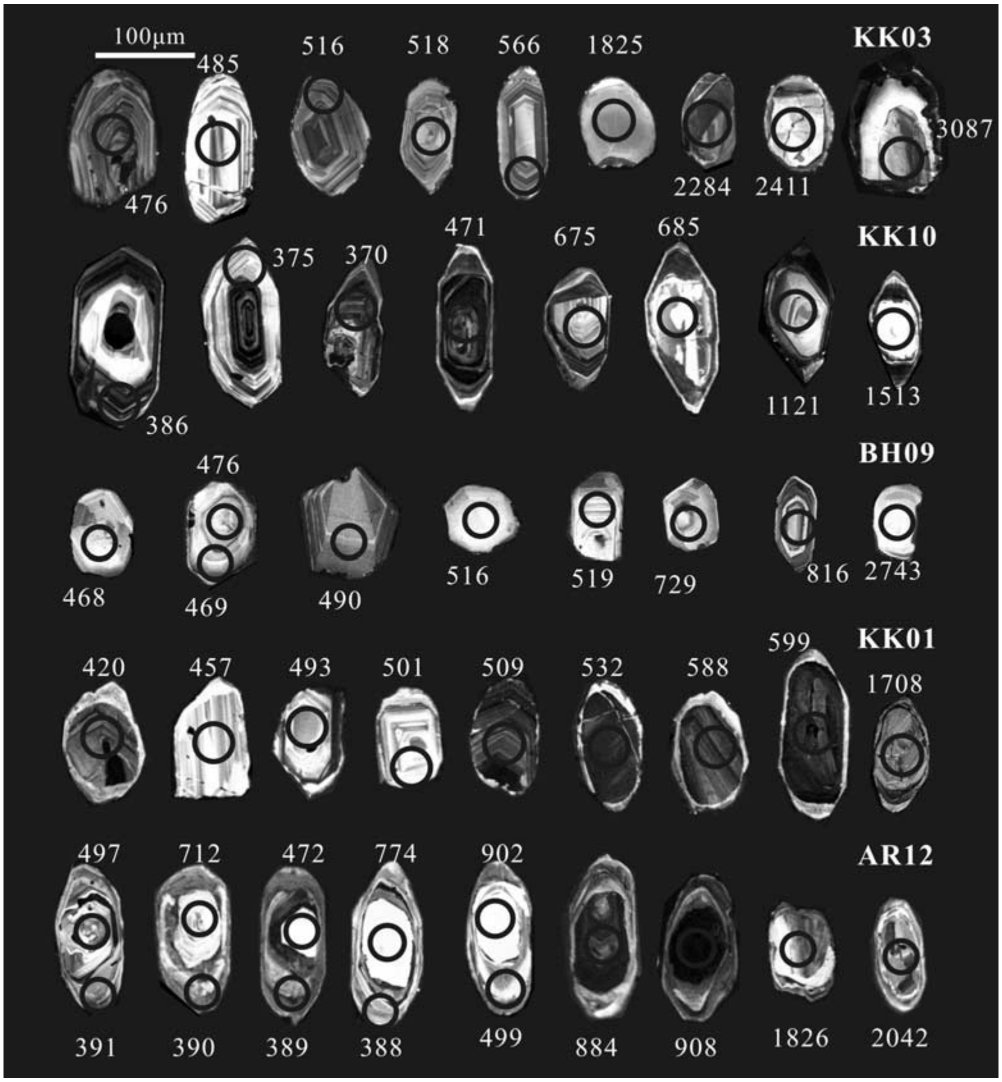

Figure 2. Representative cathodoluminescence images for detrital zircons from the Chinese Altai metasedimentary rocks. The analytical spots and crystallizing ages are indicated. The $^{206}Pb/^{238}U$ and $^{207}Pb/^{206}Pb$ ages are indicated for zircons younger than 1000 Ma and older than 1000 Ma, respectively.

5.2. Migmatite From the Habahe Group (Sample KK10)

[21] Fifty-four detrital zircons from this sample, many of them have core-rim structure, were analyzed successfully for U-Pb isotopic compositions (Figure 2). The zircon cores have oscillatory zoning and rounded shapes, indicating an erosion-transportation history. The rims are quite wide, also with oscillatory zoning and form euhedral outlines. Both zircon cores and rims have high Th/U ratios (>0.1), suggesting that the cores represent detrital zircons derived from a magmatic provenance, whereas the rims are overgrowth formed during the migmatization. Most of the analyses from this sample are discordant (Table A1), possibly owing to the effect of migmatization on the previously formed zircons. Most of the zircon cores consisted a predominant population with $^{206}Pb/^{238}U$ ages between ∼460 and 513 Ma, whereas others gave Neoproterozoic $^{206}Pb/^{238}U$ ages (659–786 Ma, 14 spots) and Mesoproterozoic $^{207}Pb/^{206}Pb$ ages (1121–1127 Ma, 2 spots). The oldest zircon core yielded a $^{207}Pb/^{206}Pb$ age of 1513 Ma (Table A1 and Figure 3). Moreover, eleven spots of zircon rims gave $^{206}Pb/^{238}U$ ages ranging from 370 Ma to 401 Ma with a mean age of 384 ± 6 Ma (MSWD = 4.3, Table A1 and Figure 3). The Gaussian probability diagram shows the most prominent peak at 457 Ma and three less prominent peaks at 382 Ma, 510 Ma and 675 Ma (Figure 4).

[22] Twenty-one of the above zircons were analyzed for Hf isotopic compositions (Table A2). Five zircon cores have negative $\varepsilon_{Hf}(t)$ values, whereas the other zircon cores or rims give positive $\varepsilon_{Hf}(t)$ values (Figure 5). Most of these zircons have Neo- to Meso-proterozoic model ages, with only a few yielding Paleoproterozoic model ages (1.8–2.1 Ga).

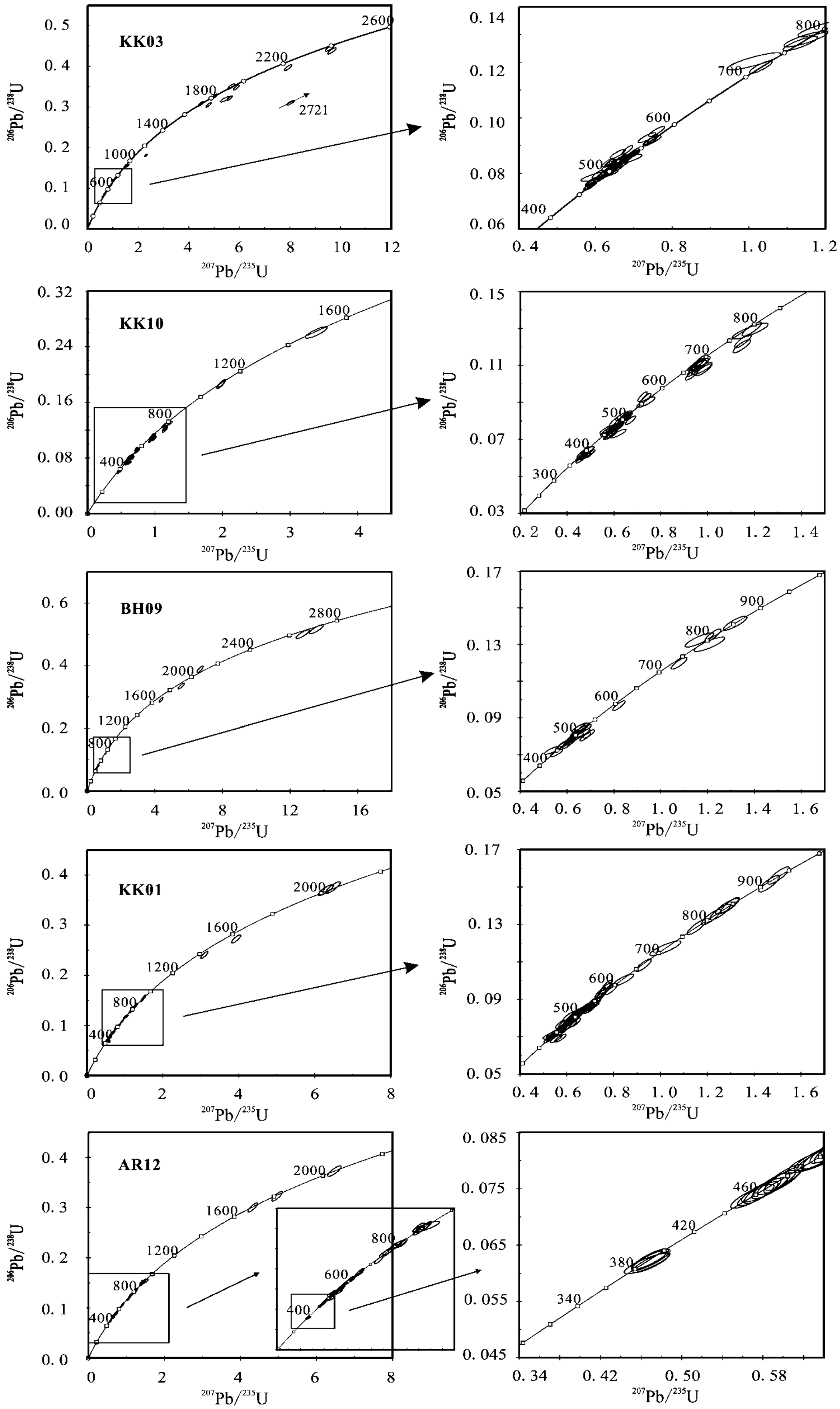

Figure 3. U-Pb concordia diagrams for detrital zircons from the Chinese Altai metasedimentary rocks.

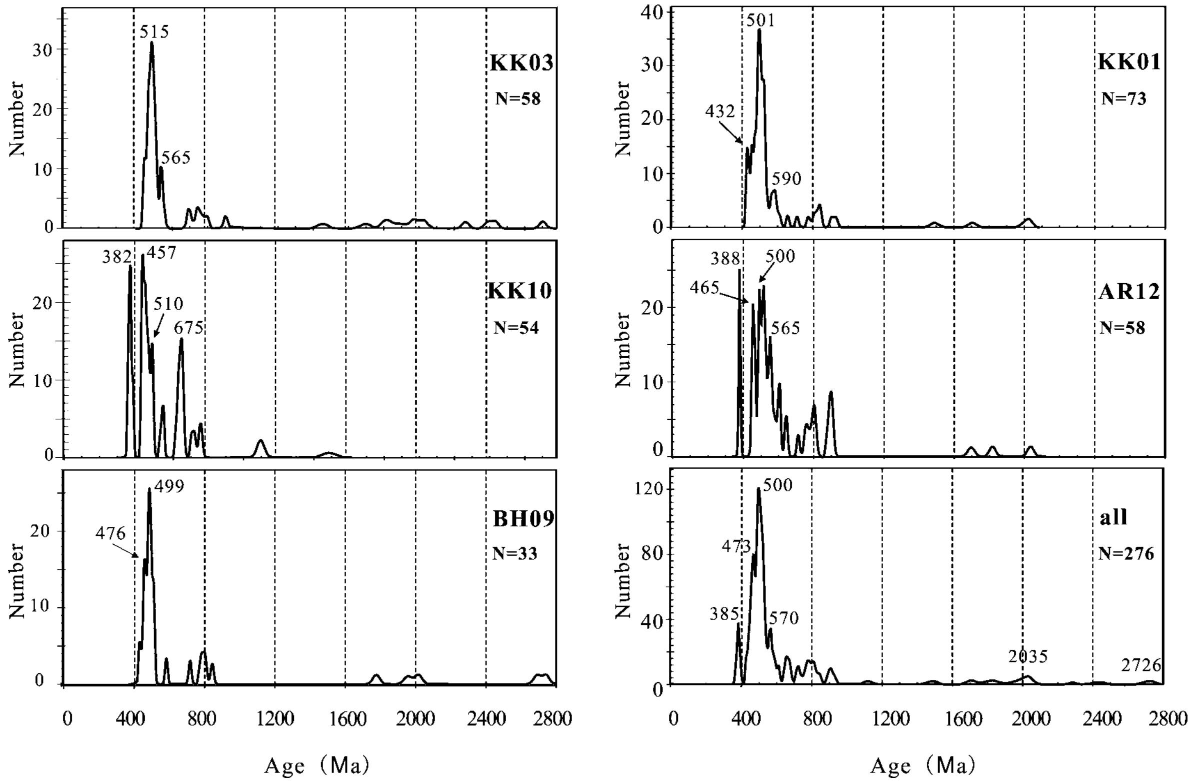

Figure 4. Age distribution of detrital zircons from the Chinese Altai metasedimentary rocks. The $^{206}Pb/^{238}U$ and $^{207}Pb/^{206}Pb$ ages are used for zircons younger than 1000 Ma and older than 1000 Ma, respectively. Each sample is shown in a separate diagram, and the last diagram shows all of the samples. See Table A1 for a list of zircon ages.

5.3. Siltstone From the Habahe Group (Sample BH09)

[23] Zircons separated from this sample are less in amount and smaller in size than those from other samples in this study, and most are subhedral to rounded with oscillatory zoning or nebulous zoning (Figure 2). Because of the small amount and small size, U-Pb isotopic data of only thirty-three spots were analyzed successfully. Most of the zircons with high Th/U ratios (>0.1) gave a predominant $^{206}Pb/^{238}U$ age population between 465 and 525 Ma, and other zircons have Proterozoic ages which scatter at 594–854 ($^{206}Pb/^{238}U$ age, 4 spots) and 1782–2021 Ma ($^{207}Pb/^{206}Pb$ age, 3 spots) (Figure 3). Two very small rounded zircon grains with bright luminescence and high Th/U ratios (0.25–0.28) yielded Archean $^{207}Pb/^{206}Pb$ ages (2693 and 2743 Ma, respectively, Figure 2). In the Gaussian probability diagram, age data of this sample show a prominent peak at 499 Ma, and a younger peak at 476 Ma (Figure 4).

[24] We analyzed twenty-five grains of these zircons for Hf isotopic compositions (Table A2). The $\varepsilon_{Hf}(t)$ values vary widely from −26 to +15, but most of the Paleozoic detrital zircons have $\varepsilon_{Hf}(t)$ values ranging from −10 to +15 (Figure 5). Although most of the grains have Neo- to Meso-proterozoic model ages, five yield Archean model ages (2.5–3.6 Ga).

5.4. Mylonite From the Kangbutiebao Formation (Sample KK01)

[25] Most zircons from this sample are well rounded with oscillatory zoning (Figure 2). Overgrowth rims are common, but too narrow to analyze. Seventy-three zircon grains were analyzed successfully for U-Pb isotopic compositions, and they mostly gave concordant or nearly concordant ages. The most predominant zircon population yielded $^{206}Pb/^{238}U$ ages between 471 and 545 Ma (41 spots, Table A1). A subordinate zircon population gave $^{206}Pb/^{238}U$ ages between 429 and 460 Ma (11 spots, Table A1). In addition, a relatively small number of zircons were derived from a Neoproterozoic provenance ($^{206}Pb/^{238}U$ age, 561–935 Ma, 15 spots), and two yielded concordant Paleoproterozoic $^{207}Pb/^{206}Pb$ ages (2005 and 2033 Ma, respectively) (Figure 3). In the Gaussian probability diagram, these data gave a prominent peak at 501 Ma, followed by a minor peak at 432 Ma (Figure 4).

[26] Twenty-nine grains from this sample were also analyzed for Hf isotopic compositions (Table A2), of which twenty have positive or zero $\varepsilon_{Hf}(t)$ values and nine have negative $\varepsilon_{Hf}(t)$ values (0 to −18) (Figure 5), indicating a significant contribution of juvenile material in the sedimentary provenance. Although one Archean model ages was obtained (3.4 Ga), other detrital zircons have Neo- to Meso-proterozoic model ages.

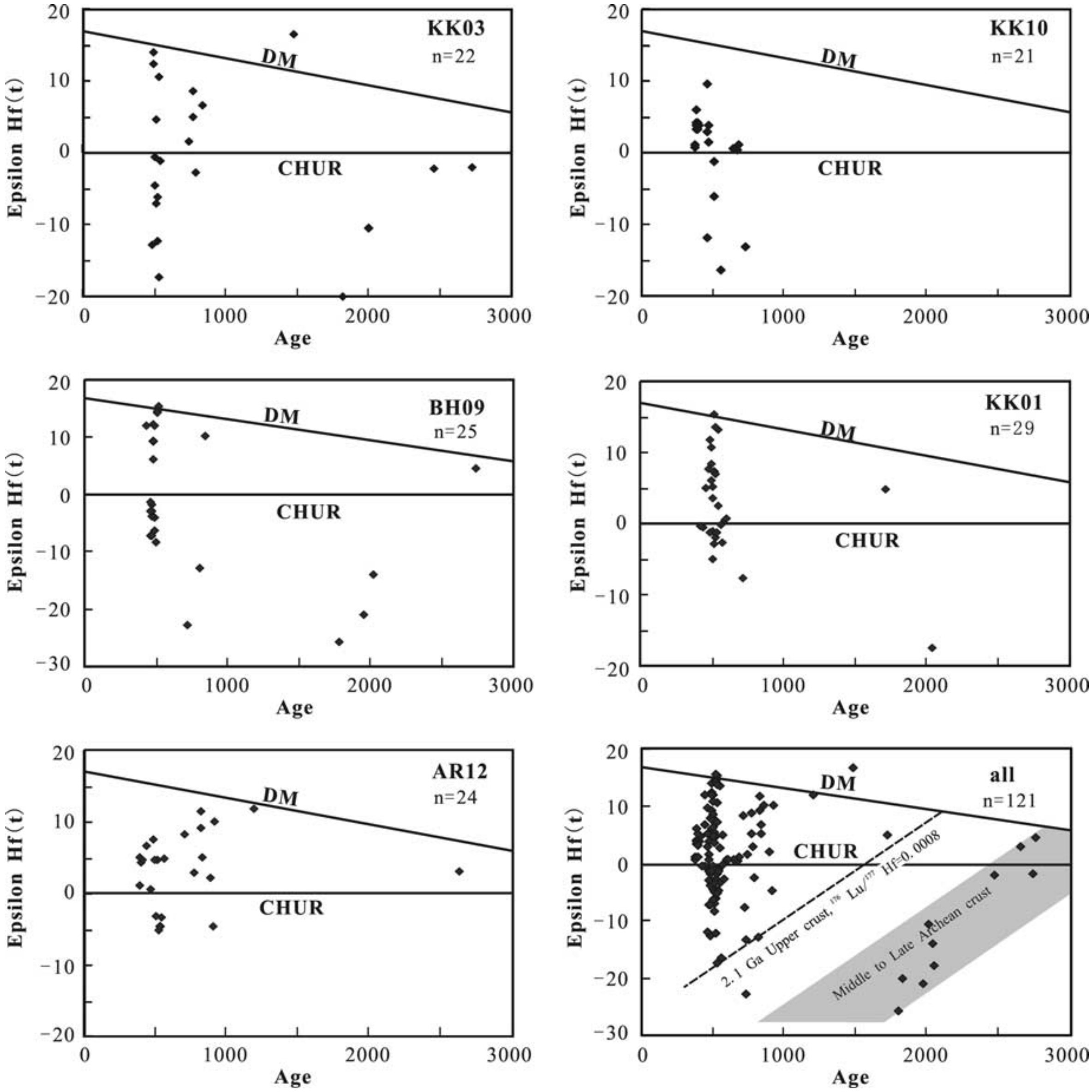

Figure 5. Diagram of ε_{Hf}(t) values versus crystallizing ages for zircons from the Chinese Altai metasedimentary rocks. The $^{206}Pb/^{238}U$ ages are used for zircons younger than 1000 Ma, and $^{207}Pb/^{206}Pb$ ages are used for zircons older than 1000 Ma.

5.5. Garnet-Sillimanite Gneiss From the Altai Formation (Sample AR12)

[27] Zircon grains separated from this sample commonly have a core-rim structure (Figure 2). Fifty-eight zircons were analyzed successfully for U-Pb isotopic compositions (Table A1), and they mostly have concordant or nearly concordant data. The predominant population of zircon cores has $^{206}Pb/^{238}U$ ages between 456 and 547 Ma, and other zircon cores mostly have Neoproterozoic $^{206}Pb/^{238}U$ ages (553–916 Ma). Three zircon cores yielded Paleoproterozoic $^{207}Pb/^{206}Pb$ ages of 1705, 1826 and 2042 Ma, respectively (Figure 3). A younger age population is defined by five analyses of zircon rims, yielding $^{206}Pb/^{238}U$ ages between 388 and 391 Ma, with a concordia age of 389 ± 2 Ma (MSWD = 1.2). Because all these younger ages were obtained from zircon rims with low Th/U ratios (0.01–0.06), we suggest that the rims formed in the Middle Devonian. In the Gaussian probability diagram, a prominent age peak at 500 Ma is followed by three small peaks at 388 Ma, 465 Ma and 565 Ma (Figure 4).

[28] Twenty-four of these zircon grains were analyzed for Hf isotopic compositions (Table A2). The ε_{Hf}(t) values vary from −5 to +12, with eighty percent of them having positive ε_{Hf}(t) values (Figure 5), indicating a significant contribution of juvenile material in the sedimentary provenance. Most of these detrital zircons have Neo- to Meso-

proterozoic model ages, but one Archean model age was also obtained (2.9 Ga).

6. Discussion

6.1. Timing of Deposition and Metamorphism

[29] Because the time of sedimentary deposition must be later than the formation of detrital zircons, the age of the youngest detrital zircon can be used to constrain the maximum age of deposition with the proviso that there was no disturbance in the U-Pb isotopic system [e.g., *Nelson*, 2001; *Williams*, 2001; *Fedo et al.*, 2003]. This approach has been successfully applied to sedimentary systems, especially to Precambrian successions where biostratigraphy cannot be used [e.g., *Bingen et al.*, 2001; *Guan et al.*, 2002; *Griffin et al.*, 2004; *Luo et al.*, 2004; *Andersen*, 2005; *Payne et al.*, 2006; *Moecher and Samson*, 2006; *Xia et al.*, 2006a]. In the Chinese Altai, the Habahe Group was originally assigned a Middle to Late Ordovician age, but recent workers have suggested a Sinian or Sinian to Middle Ordovician age [e.g., *GCRSX*, 1981; *Wang*, 1983; *Peng*, 1989; *BGMRX*, 1993; *Windley et al.*, 2002; *Chen and Jahn*, 2002; *Li et al.*, 2006]. The detrital zircons from the three Habahe metasedimentary samples studied here cluster into three distinct groups with $^{206}Pb/^{238}U$ ages between 468–541, 460–513 and 465–525 Ma, respectively. This supports the previous suggestion that the Habahe Group was not deposited prior to the Middle Ordovician. Zircons from the Kangbutiebao mylonitic sample show a large population at 471–545 Ma, with a subordinate younger population at 429–460 Ma. This implies that the deposition of the Kangbutiebao Formation was not prior to Early Silurian, consistent with the upper Silurian to lower Devonian age assigned to this formation [e.g., *Windley et al.*, 2002] and the previously published single-grain zircon TIMS U–Pb age of 407 ± 9 Ma for a meta-volcanic sample from this unit [*Zhang et al.*, 2000]. Zircons from the paragneissic sample from the Altai Formation have a predominant age population of 456–547 Ma, which is consistent with but cannot give rigorous constraint on the depositional age for this formation, because this age range is ~80 Ma older than the commonly assigned Middle Devonian age [e.g., *Windley et al.*, 2002].

[30] Zircons from both the Habahe migmatite and the Altai paragneisses have metamorphic overgrowths (Figure 2), which yielded a mean $^{206}Pb/^{238}U$ age of 384 ± 6 Ma and a U-Pb concordia age of 389 ± 2 Ma, respectively (Figure 3). The regional metamorphism in this region was thought to have occurred in the Late Devonian to Late Carboniferous, on the basis of Rb-Sr whole rock isochorn and hornblende K-Ar ages [*Ermolov*, 1984; *Zhuang*, 1994a, 1994b], or in the Early Permian, on the basis of a chemical Th-U-Pb monazite age of 262 ± 10 Ma [*Zheng et al.*, 2005]. Most recently, in the southeast part of the Central Altai domain, gneissic rocks from Qinghe yielded concordant SHRIMP U–Pb age of 281 ± 3 Ma, which was interpreted to record a major metamorphic event [*Hu et al.*, 2006]. In the Qiongkuer domain, SHRIMP U-Pb dating for four zircon samples from Wuqiagou mafic granulite gave concordant ages of 268~279 Ma, and an age of ~255 Ma for a zircon rim which was considered to represent the age of granulite facies metamorphism [*Chen et al.*, 2006]. The above data suggest that the Chinese Altai underwent multiple thermal events and complex tectonic evolutionary history, inviting further detailed study.

6.2. Sedimentary Provenance

[31] The Habahe metasedientary rocks are widely distributed in the Central Altai Domain, and are generally envisaged as passive continental margin deposits [e.g., *Chang et al.*, 1995; *Chen and Jahn*, 2002; *Li et al.*, 2006]. The high-grade metamorphic rocks in the region have been considered to represent the Precambrian basement of a microcontinent [e.g., *Windley et al.*, 2002; *Li et al.*, 2003]. Recently, *Li et al.* [2006] suggested the existence of a so-called Altai-Mongolia Precambrian microcontinent which supposedly underlies the Chinese Altai and Junggar Basin. If the above tectonic interpretations are correct, detrital zircons with Precambrian ages would be predominant in the Habahe metasedimentary rocks, as in the case of the North China Craton [*Darby and Gehrels*, 2006]. However, data from this study show an entire different picture.

[32] The detrital zircons from each of the three metasedimentary samples from the Habahe Group all have a predominant population between ~460 to ~540 Ma (Figure 4), clearly indicating that their provenance was dominated by Cambrian to Early Ordovician rocks. Zircon Hf isotopic compositions indicate that the provenance contained a significant amount of juvenile materials (Figure 5). In addition, a large number of these zircons have euhedral to subhedral shapes (e.g., Figure 2), which may imply a short transportation distance. The flysch rhythms of the sequence support an accretionary prism origin for the protolith of these metasedimentary rocks. On the basis of these lines of evidence, we propose that a Cambrian-Early Ordovian continental arc was the main source for the Habahe sedimentary rocks. This interpretation is very well consistent with our own (X. P. Long et al., Early Paleozoic sedimentary record of the Chinese Altai: implications for the tectonic evolution of the Altai orogen, submitted to *Sedimentary Geology,* 2007) and the previously published geochemical data [*Li et al.*, 2006], which clearly indicate that these sediments were derived from an active continental margin or island arc. Our recently obtained data for the high-grade metamorphic gneisses from the central Altai indicate that the gneissic rocks have granitic compositions, are characterized by high MgO, Ni and Cr, and were emplaced in a Cambrian–Early Ordovician continental arc environment (500–470 Ma [*Sun et al.*, 2006]). A gneissic granitic sample studied by *Wang et al.* [2006], which gave 462 ± 10 Ma zircon SHRIMP U-Pb age, may represent similar type of rocks. Coeval volcanic rocks in the Central Altai include rhyolite (505 ± 2 Ma zircon evaporation age [*Windley et al.*, 2002]) and dacite (475 ± 5 Ma, zircon TIMS U-Pb age [*Shan et al.*, 2005]). Because significant (although relatively small) amounts of detrital zircons from the Habahe Group have Neoproterozoic ages, we suggest that this arc was built on a young (Neoproterozoic) continental margin, which

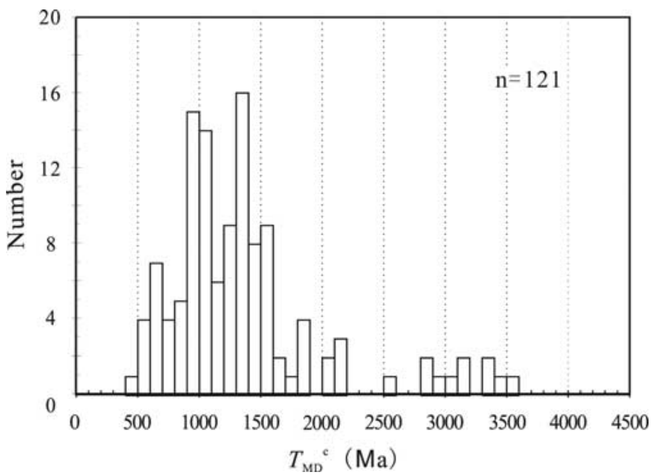

Figure 6. Histogram for the distribution of Hf model ages (T_{MD}^{c}) of zircons from the Chinese Altai metasedimentary rocks. The $^{206}Pb/^{238}U$ and $^{207}Pb/^{206}Pb$ ages are used in the calculation of the T_{MD}^{c} for zircons younger than 1000 Ma and older than 1000 Ma, respectively.

may in turn represent a Neoproterozoic arc system near or on an older continent as suggested by our predominant Neo- to Meso-proterozoic Hf model ages and sparse Paleoproterozoic to Archean detrital zircons (Figures 4 and 6). Nevertheless, our data clearly indicate that rocks of Precambrian age do not dominate the Central Altai Domain, and a passive continental margin model cannot be correct. The proposed Cambrian−Early Ordovician continental arc was possibly also a major source for the metasedimentary rocks in the Qiongkuer Domain, as manifested by the indistinguishable predominant zircon age population (Figure 4).

6.3. Implications for the Tectonic Evolution

[33] The tectonic evolutionary history of the Chinese Altai is currently hotly debated, as represented by two extreme models, i.e., the open-closure versus arc accretion models [e.g., *Huang et al.*, 1990; *He et al.*, 1990; *Xiao et al.*, 1990; *Sengör et al.*, 1993; *Chen et al.*, 1997; *Li and Poliyangsiji*, 2001; *Windley et al.*, 2002; *Xiao et al.*, 2003, 2004]. The traditional open-closure model proposes the existence of a Precambrian continent in the Junggar or Junggar-Altai region [e.g., *He et al.*, 1990; *Huang et al.*, 1990; *Xiao et al.*, 1990, 1992; *Berzin and Dobretsov*, 1993; *Li*, 1991; *Yuan*, 1995; *Liu et al.*, 1998; *Li and Poliyangsiji*, 2001], and envisages that the Early Paleozoic sedimentary rocks were deposited on a passive continental margin without significant contribution from magmatic activities until the continent collided with the Siberian Plate in the Middle or Late Ordovician [*He et al.*, 1990; *Li and Poliyangsiji*, 2001; *Li et al.*, 2006]. Recent studies do not support the existence of a continental basement under the Junggar basin [e.g., *Zhou*, 1994; *Han et al.*, 1997; *F. Z. Wang et al.*, 2002; *Hu and Wei*, 2003; *Chen and Jahn*, 2004; *Yuan et al.*, 2006; *Long et al.*, 2006]. This study shows that large amounts of detrital zircons were crystallized in the Early Paleozoic arc magmas derived from mantle or crustal sources. Therefore our data favor an arc accretionary history, and do not support the microcontinent model. Recent Pb isotopic data for magmatic and sedimentary rocks and ore deposits show dominant juvenile characteristics for the Chinese Altai [*Chiaradia et al.*, 2006], also consistent with our interpretation.

[34] Recently, numerous U-Pb ages for detrital zircons from the Siberia Craton, North China Craton and Tarim Craton have been published [e.g., *Darby and Gehrels*, 2006; *Lu et al.*, 2006; *Zhao et al.*, 2005; *Khudoley et al.*, 2001; *Rainbird et al.*, 1998]. For the North China Craton, the main peaks of magmatic events are 2.9−2.7, 2.6−2.45 and 2.35−1.95 Ga, and two important metamorphic-magmatic events at 2.6−2.4 Ga and 1.9−1.8 Ga are also defined [*Wan et al.*, 2006; *Kröner et al.*, 2005; *Wilde and Zhao*, 2005; *Zhai and Liu*, 2003; *Zhao et al.*, 2000; *Zhang et al.*, 1996]. Expect for a few magmatic rocks having ages of 1.3−1.0 Ga or 0.80−0.65 Ga, the North China Craton was tectonically stable from 1.65 to 0.16 Ga [*Zhai et al.*, 2003]. Magmatic events have been revealed on the Siberia platform by detrital zircon ages mainly at ∼3.4−2.6 Ga and 2.2−1.7 Ga, and younger Mesoproterozoic magmatic events (<∼1.7 Ga) are not reported [*Bibikova et al.*, 1981; *Frost et al.*, 1998; *Jahn et al.*, 1998; *Ross and Villeneuve*, 1998; *Kuzmin et al.*, 1995; *Bruguier*, 1996; *Khudoley et al.*, 2001]. Several Neoproterozoic magmatic arcs occur along the southeastern margin of Siberia Craton, with age peaks of zircons at 880−860, ∼800, 760−720, 700−630 and 536−464 Ma [*Rainbird et al.*, 1998; *Khudoley et al.*, 2001; *Salnikova et al.*, 2001; *Vernikovskaya et al.*, 2002; *Vernikovsky et al.*, 2002, 2003; *Khain et al.*, 2003; *Wilde et al.*, 2000, 2003; *Kuzmichev et al.*, 2001, 2005; *Gladkochub et al.*, 2006]. Although recent studies have shown that the basement of the Tarim Craton mainly formed between 2.3−2.6 Ga with later granites intruded at 1.94 Ga, and that some Neoproterozoic volcanic rocks (700−800 Ma) occur on the margin of this craton [*Guo et al.*, 2003; *Xu et al.*, 2005; *Zhang et al.*, 2006; *Hu and Wei*, 2006], Neoproterozoic magmatic events are rare compared to the magmatic arcs along the southeastern margin of Siberia Craton. The existence of Ordovician ophiolites in the south margin of the Chinese Altai orogen but not in its north margin [*Xiao et al.*, 2006; *Wang et al.*, 2003; *Khain et al.*, 2003], suggests that the significant Neoproterozoic zircons from the Chinese Altai (Figure 4) were derived from the Neoproterozoic magmatic arcs near the southeastern margin of Siberia Craton, with older zircons from a more distal source in the craton.

[35] The diagram of $\varepsilon_{Hf}(t)$ versus crystallizing age clearly shows that two important crustal accretion events occurred in the Early Paleozoic and Neoproterozoic in the Chinese Altai (Figure 5). Many of detrital zircons have positive $\varepsilon_{Hf}(t)$ values, indicating the addition of voluminous juvenile materials to the crust in these two periods. Some Paleoproterozoic and Archean detrital zircons have also been identified in this study. Although their $\varepsilon_{Hf}(t)$ values vary from −26 to +3, data show a narrow $\varepsilon_{Hf}(t)$ evolutionary trend projecting to Archean model ages (Figure 5). This may imply significant reworking of Archean crustal materials in

Table A1. U-Pb Data for Zircons From the Chinese Altai Metasedimentary Rocks[a]

Sample Spot	Ratios							Ages, Ma						
	Th/U	Pb^{207}/Pb^{206}	1σ	Pb^{207}/U^{235}	1σ	Pb^{206}/U^{238}	1σ	Pb^{207}/Pb^{206}	1σ	Pb^{206}/U^{238}	1σ	Pb^{207}/U^{235}	1σ	Disc%
KK03: Habahe Schist														
1	0.23	0.05759	0.00090	0.66223	0.01079	0.08334	0.00101	514	34	516	6	516	7	0
2	0.25	0.05901	0.00120	0.74763	0.01538	0.09184	0.00116	567	44	566	7	567	9	0
3	0.39	0.05788	0.00101	0.75922	0.01366	0.09507	0.00117	525	38	586	7	574	8	−12
4	0.12	0.05890	0.00068	0.74940	0.00943	0.09222	0.00109	564	25	569	6	568	5	−1
5	0.28	0.05718	0.00070	0.63316	0.00839	0.08027	0.00095	498	27	498	6	498	5	0
6	0.14	0.05767	0.00274	0.67388	0.03136	0.08470	0.00140	517	101	524	8	523	19	−1
7	0.28	0.15588	0.00176	9.57547	0.11861	0.44527	0.00534	2411	19	2374	24	2395	11	2
8	0.26	0.06532	0.00230	1.19121	0.04140	0.13219	0.00196	785	72	800	11	797	19	−2
9	0.41	0.05662	0.00120	0.65350	0.01402	0.08366	0.00106	476	47	518	6	511	9	−9
10	0.35	0.14469	0.00162	7.92753	0.09762	0.39714	0.00475	2284	19	2156	22	2223	11	6
11	0.27	0.05669	0.00087	0.66619	0.01062	0.08518	0.00103	479	34	527	6	518	6	−10
12	0.28	0.09239	0.00142	2.31024	0.03674	0.18126	0.00224	1475	29	1074	12	1215	11	27
13	0.17	0.05484	0.00107	0.65777	0.01305	0.08694	0.00108	406	43	537	6	513	8	−32
14	0.18	0.05474	0.00092	0.63353	0.01104	0.08390	0.00103	402	37	519	6	498	7	−29
15	0.21	0.15972	0.00166	9.65977	0.11247	0.43839	0.00518	2453	18	2343	23	2403	11	4
16	0.44	0.06660	0.00152	1.25718	0.02873	0.13683	0.00178	825	47	827	10	827	13	0
17	0.55	0.05687	0.00083	0.66817	0.01023	0.08517	0.00103	486	32	527	6	520	6	−8
18	0.23	0.05578	0.00110	0.63483	0.01274	0.08250	0.00103	443	43	511	6	499	8	−15
19	0.33	0.05733	0.00117	0.73430	0.01513	0.09284	0.00117	504	45	572	7	559	9	−14
20	0.47	0.05766	0.00157	0.65798	0.01778	0.08272	0.00110	517	59	512	7	513	11	1
21	0.23	0.05628	0.00098	0.58418	0.01043	0.07524	0.00092	463	38	468	6	467	7	−1
22	0.21	0.05780	0.00088	0.67160	0.01071	0.08422	0.00102	522	33	521	6	522	7	0
23	0.48	0.10541	0.00148	4.47915	0.06619	0.30800	0.00379	1722	26	1731	19	1727	12	−1
24	0.35	0.05654	0.00089	0.64040	0.01046	0.08210	0.00100	473	35	509	6	503	6	−8
25	0.56	0.05738	0.00073	0.64428	0.00877	0.08139	0.00097	506	28	504	6	505	5	0
26	0.53	0.06488	0.00171	1.13458	0.02970	0.12676	0.00170	770	54	769	10	770	14	0
27	0.30	0.05591	0.00112	0.59118	0.01200	0.07664	0.00096	449	44	476	6	472	8	−6
28	0.11	0.11357	0.00152	4.78285	0.06787	0.30527	0.00372	1857	24	1717	18	1782	12	8
29	0.27	0.05518	0.00079	0.63713	0.00959	0.08370	0.00101	419	31	518	6	501	6	−24
30	0.24	0.05889	0.00081	0.74248	0.01083	0.09148	0.00110	563	30	564	7	564	6	0
31	0.07	0.18753	0.00204	8.02097	0.09700	0.31037	0.00370	2721	18	1743	18	2233	11	36
32	0.18	0.05815	0.00082	0.70214	0.01046	0.08762	0.00106	535	31	541	6	540	6	−1
33	0.36	0.12351	0.00276	5.42923	0.12078	0.31898	0.00450	2008	39	1785	22	1890	19	11
34	0.16	0.12659	0.00143	5.62058	0.06983	0.32218	0.00384	2051	20	1800	19	1919	11	12
35	0.33	0.05736	0.00072	0.64608	0.00878	0.08173	0.00098	505	27	507	6	506	5	0
36	0.14	0.05606	0.00069	0.68346	0.00913	0.08847	0.00105	454	27	547	6	529	6	−20
37	0.16	0.11157	0.00141	5.01700	0.06825	0.32630	0.00395	1825	23	1820	19	1822	12	0
38	0.39	0.05736	0.00173	0.64141	0.01920	0.08114	0.00111	505	65	503	7	503	12	0
39	0.25	0.05752	0.00110	0.65776	0.01281	0.08298	0.00103	511	42	514	6	513	8	−1
40	0.24	0.05544	0.00081	0.58709	0.00904	0.07685	0.00093	430	32	477	6	469	6	−11
41	0.86	0.05675	0.00102	0.61130	0.01128	0.07816	0.00097	481	40	485	6	484	7	−1
42	0.40	0.06970	0.00083	1.49402	0.01951	0.15554	0.00185	920	24	932	10	928	8	−1
43	0.32	0.05736	0.00076	0.63557	0.00904	0.08041	0.00096	505	29	499	6	500	6	1
44	0.08	0.12257	0.00144	5.88078	0.07559	0.34816	0.00418	1994	21	1926	20	1958	11	3
45	0.39	0.07281	0.00280	1.55676	0.05874	0.15515	0.00247	1009	76	930	14	953	23	8
46	1.54	0.11747	0.00183	5.67331	0.09152	0.35045	0.00442	1918	28	1937	21	1927	14	−1
47	0.14	0.05827	0.00098	0.69729	0.01216	0.08684	0.00107	539	37	537	6	537	7	0
48	0.64	0.06494	0.00217	1.14923	0.03794	0.12842	0.00186	772	69	779	11	777	18	−1
49	0.24	0.05783	0.00124	0.68588	0.01488	0.08606	0.00109	523	47	532	6	530	9	−2
50	0.26	0.05726	0.00089	0.62827	0.01021	0.07963	0.00097	501	34	494	6	495	6	1
51	0.21	0.05809	0.00079	0.68467	0.00987	0.08552	0.00103	533	30	529	6	530	6	1
52	0.30	0.05515	0.00079	0.60556	0.00918	0.07968	0.00096	418	32	494	6	481	6	−18
53	0.36	0.23512	0.00299	19.45708	0.26510	0.60050	0.00751	3087	20	3032	30	3065	13	2
54	0.24	0.05593	0.00300	0.61047	0.03216	0.07920	0.00136	449	115	491	8	484	20	−9
55	0.43	0.06112	0.00285	1.01412	0.04639	0.12039	0.00202	644	97	733	12	711	23	−14
56	0.62	0.05629	0.00101	0.58798	0.01081	0.07580	0.00094	463	39	471	6	470	7	−2
57	0.85	0.06328	0.00117	1.03155	0.01955	0.11829	0.00148	718	39	721	9	720	10	0
58	0.60	0.05708	0.00148	0.62901	0.01634	0.07997	0.00105	494	57	496	6	496	10	0
KK10: Habahe Migmatite														
1	0.22	0.05509	0.00137	0.48648	0.01212	0.06402	0.00083	416	54	400	5	403	8	4
2	0.42	0.06053	0.00074	0.67083	0.00896	0.08034	0.00096	623	26	498	6	521	5	20
3	0.23	0.05628	0.00133	0.47225	0.01119	0.06083	0.00078	463	52	381	5	393	8	18
4	0.50	0.06626	0.00086	0.98394	0.01375	0.10766	0.00129	814	27	659	7	696	7	19
5	0.20	0.06352	0.00093	0.95905	0.01488	0.10946	0.00132	726	31	670	8	683	8	8
6	0.29	0.05608	0.00089	0.45633	0.00759	0.05899	0.00072	455	35	370	4	382	5	19

Table A1. (continued)

		Ratios						Ages, Ma						
Sample Spot	Th/U	Pb^{207}/Pb^{206}	1σ	Pb^{207}/U^{235}	1σ	Pb^{206}/U^{238}	1σ	Pb^{207}/Pb^{206}	1σ	Pb^{206}/U^{238}	1σ	Pb^{207}/U^{235}	1σ	Disc%
7	0.17	0.05745	0.00070	0.59359	0.00786	0.07490	0.00089	509	26	466	5	473	5	8
8	0.26	0.06301	0.00115	0.95915	0.01804	0.11036	0.00137	708	39	675	8	683	9	5
9	0.32	0.05375	0.00068	0.45710	0.00627	0.06166	0.00073	360	28	386	4	382	4	−7
10	0.22	0.05624	0.00086	0.59004	0.00950	0.07606	0.00092	461	34	473	6	471	6	−2
11	0.23	0.05746	0.00068	0.65116	0.00842	0.08216	0.00097	509	26	509	6	509	5	0
12	0.24	0.06354	0.00083	0.97776	0.01376	0.11157	0.00133	726	28	682	8	693	7	6
13	0.60	0.05690	0.00077	0.59475	0.00864	0.07578	0.00091	487	30	471	5	474	6	3
14	0.35	0.05542	0.00082	0.56498	0.00883	0.07391	0.00089	429	32	460	5	455	6	−7
15	0.21	0.05726	0.00070	0.59794	0.00795	0.07571	0.00090	501	27	471	5	476	5	6
16	0.28	0.05749	0.00107	0.49567	0.00947	0.06251	0.00077	510	41	391	5	409	6	23
17	0.15	0.06126	0.00138	0.61749	0.01402	0.07308	0.00094	648	48	455	6	488	9	30
18	0.27	0.06252	0.00072	0.95280	0.01208	0.11049	0.00131	692	24	676	8	680	6	2
19	0.42	0.05867	0.00107	0.58520	0.01100	0.07231	0.00089	555	39	450	5	468	7	19
20	0.10	0.06336	0.00103	0.96489	0.01634	0.11040	0.00135	721	34	675	8	686	8	6
21	0.53	0.06663	0.00177	1.18155	0.03134	0.12855	0.00174	826	55	780	10	792	15	6
22	0.30	0.06645	0.00088	1.18860	0.01685	0.12968	0.00155	821	27	786	9	795	8	4
23	0.21	0.05485	0.00113	0.56926	0.01189	0.07524	0.00094	406	45	468	6	458	8	−15
24	0.28	0.05523	0.00095	0.46110	0.00818	0.06053	0.00074	421	37	379	5	385	6	10
25	0.60	0.05690	0.00094	0.47714	0.00817	0.06079	0.00074	487	36	380	5	396	6	22
26	0.60	0.05615	0.00124	0.64141	0.01434	0.08282	0.00105	458	48	513	6	503	9	−12
27	0.78	0.06537	0.00115	0.97651	0.01763	0.10830	0.00134	786	36	663	8	692	9	16
28	0.20	0.09426	0.00180	3.38695	0.06577	0.26049	0.00337	1513	36	1492	17	1501	15	1
29	0.39	0.05786	0.00064	0.73496	0.00905	0.09211	0.00109	524	24	568	6	560	5	−8
30	0.19	0.07698	0.00078	1.98734	0.02310	0.18721	0.00222	1121	20	1106	12	1111	8	1
31	0.10	0.06250	0.00065	0.96622	0.01139	0.11210	0.00133	691	22	685	8	687	6	1
32	0.18	0.05769	0.00058	0.62622	0.00720	0.07870	0.00093	518	21	488	6	494	4	6
33	0.14	0.05864	0.00064	0.62465	0.00761	0.07724	0.00092	554	23	480	5	493	5	13
34	0.25	0.05749	0.00058	0.62239	0.00721	0.07850	0.00093	510	22	487	6	491	5	4
35	0.13	0.06441	0.00073	0.93377	0.01177	0.10512	0.00125	755	24	644	7	670	6	15
36	0.13	0.06777	0.00078	1.15090	0.01461	0.12315	0.00147	861	24	749	8	778	7	13
37	0.25	0.05407	0.00064	0.47808	0.00623	0.06412	0.00076	374	27	401	5	397	4	−7
38	0.30	0.05506	0.00063	0.46706	0.00592	0.06151	0.00073	415	25	385	4	389	4	7
39	0.32	0.05480	0.00062	0.59871	0.00756	0.07923	0.00094	404	25	492	6	476	5	−22
40	0.19	0.05626	0.00056	0.72191	0.00830	0.09305	0.00110	462	22	574	6	552	5	−24
41	0.20	0.05804	0.00076	0.57543	0.00811	0.07189	0.00086	531	29	448	5	462	5	16
42	0.12	0.05929	0.00125	0.73651	0.01581	0.09008	0.00115	578	45	556	7	560	9	4
43	0.06	0.07723	0.00081	1.97206	0.02353	0.18516	0.00220	1127	21	1095	12	1106	8	3
44	0.13	0.05679	0.00076	0.64190	0.00923	0.08196	0.00099	483	30	508	6	504	6	−5
45	0.21	0.05702	0.00064	0.57730	0.00718	0.07341	0.00087	492	25	457	5	463	5	7
46	0.22	0.05854	0.00072	0.59740	0.00806	0.07399	0.00089	550	27	460	5	476	5	16
47	0.31	0.05867	0.00066	0.58941	0.00736	0.07285	0.00087	555	24	453	5	471	5	18
48	0.27	0.05823	0.00065	0.62005	0.00771	0.07721	0.00092	538	25	480	6	490	5	11
49	0.15	0.05793	0.00073	0.65646	0.00896	0.08216	0.00098	527	28	509	6	512	5	3
50	0.38	0.05811	0.00072	0.49642	0.00668	0.06195	0.00074	533	27	388	5	409	5	27
51	0.17	0.06361	0.00067	0.94054	0.01123	0.10721	0.00127	729	22	657	7	673	6	10
52	0.12	0.05879	0.00085	0.58699	0.00902	0.07240	0.00088	559	31	451	5	469	6	19
53	0.31	0.06904	0.00084	1.14613	0.01520	0.12038	0.00144	900	25	733	8	775	7	19
54	0.24	0.05463	0.00065	0.45162	0.00590	0.05994	0.00071	397	26	375	4	378	4	5
						BH09: Habahe Siltstone								
1	0.26	0.05818	0.0007	0.61974	0.00759	0.07727	0.00083	536	27	480	5	490	5	10
2	0.18	0.06534	0.00082	1.07838	0.01378	0.11973	0.00129	785	26	729	7	743	7	7
3	0.26	0.05621	0.00068	0.63169	0.00781	0.08152	0.00087	460	27	505	5	497	5	−10
4	0.34	0.05658	0.00069	0.61522	0.00765	0.07887	0.00085	475	27	489	5	487	5	−3
5	0.25	0.05918	0.00112	0.66759	0.01257	0.08183	0.00093	574	41	507	6	519	8	12
6	0.32	0.06572	0.00074	1.22252	0.01409	0.13494	0.00144	798	23	816	8	811	6	−2
7	0.31	0.05572	0.0007	0.57934	0.00736	0.07542	0.00081	441	27	469	5	464	5	−6
8	0.40	0.05707	0.00071	0.60332	0.00763	0.0767	0.00082	494	28	476	5	479	5	3
9	0.31	0.05676	0.00072	0.62894	0.00807	0.08039	0.00087	481	28	498	5	495	5	−4
10	0.53	0.0579	0.00078	0.60058	0.00813	0.07524	0.00081	526	29	468	5	478	5	11
11	0.14	0.05686	0.00069	0.60375	0.00751	0.07702	0.00083	486	27	478	5	480	5	1
12	0.17	0.05747	0.00066	0.62557	0.00738	0.07896	0.00084	509	25	490	5	493	5	4
13	0.23	0.05732	0.00066	0.63662	0.00752	0.08057	0.00086	503	25	500	5	500	5	1
14	0.25	0.10897	0.00116	4.36747	0.04803	0.29076	0.0031	1782	19	1645	16	1706	9	8
15	0.21	0.05723	0.00084	0.6575	0.00965	0.08334	0.00091	500	32	516	5	513	6	−3
16	0.40	0.05578	0.00079	0.57563	0.00823	0.07486	0.00081	443	31	465	5	462	5	−5
17	0.28	0.0675	0.00105	1.318	0.02053	0.14164	0.00157	853	32	854	9	854	9	0
18	0.12	0.12446	0.00137	6.67395	0.07777	0.38868	0.00431	2021	19	2117	20	2069	10	−5

Table A1. (continued)

	Ratios							Ages, Ma						
Sample Spot	Th/U	Pb^{207}/Pb^{206}	1σ	Pb^{207}/U^{235}	1σ	Pb^{206}/U^{238}	1σ	Pb^{207}/Pb^{206}	1σ	Pb^{206}/U^{238}	1σ	Pb^{207}/U^{235}	1σ	Disc%
19	0.77	0.06177	0.00086	0.69316	0.00995	0.08133	0.00092	666	30	504	5	535	6	24
20	0.23	0.05912	0.00109	0.66599	0.01235	0.08166	0.00095	571	40	506	6	518	8	11
21	0.70	0.06729	0.00149	1.20768	0.02652	0.13009	0.0016	847	45	788	9	804	12	7
22	0.71	0.05729	0.00082	0.67071	0.00986	0.08486	0.00096	502	31	525	6	521	6	−5
23	0.38	0.06373	0.00137	1.1648	0.02482	0.13247	0.0016	733	45	802	9	784	12	−9
24	0.15	0.05765	0.00131	0.66644	0.01504	0.08379	0.00102	516	49	519	6	519	9	−1
25	0.21	0.05611	0.00122	0.65551	0.01423	0.08468	0.00102	456	48	524	6	512	9	−15
26	0.28	0.19008	0.00228	13.5381	0.16906	0.51625	0.00586	2743	20	2683	25	2718	12	2
27	0.25	0.18442	0.00224	12.73777	0.16088	0.50063	0.0057	2693	20	2617	24	2661	12	3
28	0.39	0.05386	0.00144	0.53825	0.01421	0.07244	0.00091	365	59	451	5	437	9	−24
29	0.36	0.06159	0.00081	0.6776	0.00922	0.07974	0.0009	660	28	495	5	525	6	25
30	0.29	0.06163	0.00077	0.82124	0.01069	0.09658	0.00108	661	27	594	6	609	6	10
31	0.53	0.05849	0.00099	0.64297	0.01096	0.07968	0.00092	548	36	494	5	504	7	10
32	0.29	0.05671	0.0011	0.55408	0.01078	0.07081	0.00083	480	43	441	5	448	7	8
33	0.31	0.12042	0.00158	5.56452	0.07503	0.33494	0.00383	1962	23	1862	18	1911	12	5
KK01: Kangbutiebao Mylonite														
1	0.23	0.05825	0.00084	0.69026	0.01060	0.08596	0.00105	538	32	532	6	533	6	1
2	0.21	0.05746	0.00063	0.77168	0.00955	0.09741	0.00116	509	24	599	7	581	5	−18
3	0.22	0.06002	0.00103	0.57257	0.01020	0.06920	0.00086	604	37	431	5	460	7	29
4	0.11	0.05649	0.00110	0.59029	0.01179	0.07580	0.00095	471	43	471	6	471	8	0
5	0.18	0.05842	0.00103	0.55491	0.01015	0.06890	0.00086	546	38	430	5	448	7	21
6	0.16	0.05747	0.00073	0.64989	0.00894	0.08203	0.00099	509	27	508	6	508	6	0
7	0.24	0.06085	0.00129	0.84102	0.01812	0.10026	0.00129	634	45	616	8	620	10	3
8	0.31	0.05600	0.00075	0.62516	0.00897	0.08097	0.00098	452	29	502	6	493	6	−11
9	0.19	0.05632	0.00089	0.62527	0.01035	0.08054	0.00099	464	35	499	6	493	6	−8
10	0.19	0.05629	0.00089	0.57001	0.00941	0.07346	0.00090	463	35	457	5	458	6	1
11	0.05	0.05965	0.00071	0.63880	0.00834	0.07768	0.00093	591	25	482	6	502	5	18
12	0.07	0.05844	0.00168	0.69026	0.01978	0.08567	0.00117	547	62	530	7	533	12	3
13	0.19	0.05542	0.00099	0.52622	0.00974	0.06888	0.00086	429	39	429	5	429	6	0
14	0.11	0.06996	0.00078	1.46349	0.01816	0.15173	0.00181	927	23	911	10	915	7	2
15	0.32	0.05859	0.00102	0.61560	0.01111	0.07621	0.00095	552	38	474	6	487	7	14
16	0.20	0.05430	0.00080	0.57426	0.00899	0.07671	0.00093	383	33	477	6	461	6	−24
17	0.15	0.05569	0.00089	0.53665	0.00899	0.06990	0.00086	440	35	436	5	436	6	1
18	0.28	0.05619	0.00122	0.56840	0.01254	0.07338	0.00094	459	48	457	6	457	8	1
19	0.16	0.06708	0.00074	1.29729	0.01605	0.14029	0.00168	840	23	846	9	845	7	−1
20	0.53	0.06991	0.00079	1.50434	0.01889	0.15609	0.00187	926	23	935	10	932	8	−1
21	0.38	0.05780	0.00080	0.59447	0.00877	0.07460	0.00090	522	30	464	5	474	6	11
22	0.42	0.05777	0.00067	0.66594	0.00852	0.08361	0.00100	521	25	518	6	518	5	1
23	0.16	0.05710	0.00070	0.63587	0.00854	0.08078	0.00097	495	27	501	6	500	5	−1
24	0.92	0.12334	0.00148	6.29003	0.08262	0.36991	0.00449	2005	21	2029	21	2017	12	−1
25	0.25	0.05696	0.00074	0.62054	0.00876	0.07902	0.00095	490	29	490	6	490	5	0
26	0.05	0.06671	0.00100	1.28429	0.02021	0.13964	0.00171	829	31	843	10	839	9	−2
27	0.17	0.05708	0.00075	0.62356	0.00881	0.07924	0.00096	494	29	492	6	492	6	1
28	0.39	0.09324	0.00107	3.09490	0.03942	0.24076	0.00289	1493	22	1391	15	1431	10	7
29	0.28	0.05621	0.00123	0.56927	0.01264	0.07346	0.00094	460	48	457	6	458	8	1
30	0.29	0.05518	0.00075	0.58417	0.00848	0.07679	0.00093	419	30	477	6	467	5	−14
31	0.14	0.05785	0.00082	0.66356	0.01006	0.08319	0.00103	524	31	515	6	517	6	2
32	0.18	0.05722	0.00078	0.63686	0.00938	0.08072	0.00099	500	30	500	6	500	6	0
33	0.24	0.05605	0.00085	0.63722	0.01025	0.08246	0.00102	454	33	511	6	501	6	−13
34	0.36	0.05474	0.00106	0.53933	0.01075	0.07145	0.00091	402	42	445	5	438	7	−11
35	0.27	0.05672	0.00119	0.59918	0.01288	0.07661	0.00099	480	46	476	6	477	8	1
36	0.04	0.05717	0.00077	0.62897	0.00917	0.07978	0.00098	498	30	495	6	496	6	1
37	0.14	0.05745	0.00080	0.64783	0.00972	0.08178	0.00101	508	30	507	6	507	6	0
38	0.22	0.05540	0.00101	0.53794	0.01016	0.07042	0.00089	428	40	439	5	437	7	−2
39	0.31	0.06661	0.00085	1.25474	0.01797	0.13662	0.00172	826	27	826	10	826	8	0
40	0.46	0.06222	0.00081	0.92763	0.01347	0.10814	0.00136	682	28	662	8	666	7	3
41	0.37	0.06515	0.00083	1.15406	0.01642	0.12848	0.00161	779	27	779	9	779	8	0
42	0.36	0.05775	0.00081	0.66858	0.01024	0.08398	0.00106	520	31	520	6	520	6	0
43	0.33	0.05779	0.00096	0.67283	0.01185	0.08445	0.00108	522	36	523	6	522	7	0
44	0.38	0.05789	0.00064	0.68085	0.00876	0.08531	0.00106	525	24	528	6	527	5	0
45	0.35	0.05808	0.00104	0.68675	0.01286	0.08576	0.00111	532	39	530	7	531	8	0
46	0.23	0.06009	0.00070	0.79120	0.01053	0.09550	0.00119	607	25	588	7	592	6	3
47	0.48	0.06590	0.00080	1.21642	0.01675	0.13387	0.00167	803	25	810	10	808	8	−1
48	0.31	0.05807	0.00073	0.63621	0.00902	0.07947	0.00099	532	28	493	6	500	6	7
49	0.28	0.05580	0.00063	0.60683	0.00790	0.07888	0.00098	444	24	489	6	482	5	−10
50	0.46	0.05928	0.00068	0.69482	0.00920	0.08502	0.00106	577	25	526	6	536	6	9
51	0.17	0.05562	0.00203	0.54733	0.01987	0.07137	0.00107	437	79	444	6	443	13	−2

Table A1. (continued)

	Ratios							Ages, Ma						
Sample Spot	Th/U	Pb^{207}/Pb^{206}	1σ	Pb^{207}/U^{235}	1σ	Pb^{206}/U^{238}	1σ	Pb^{207}/Pb^{206}	1σ	Pb^{206}/U^{238}	1σ	Pb^{207}/U^{235}	1σ	Disc%
52	0.01	0.05796	0.00078	0.76442	0.01133	0.09566	0.00120	528	29	589	7	577	7	−12
53	0.22	0.05652	0.00085	0.61782	0.01007	0.07928	0.00100	472	33	492	6	489	6	−4
54	0.24	0.05784	0.00067	0.74427	0.00987	0.09333	0.00116	523	25	575	7	565	6	−10
55	0.27	0.05838	0.00066	0.71033	0.00927	0.08826	0.00110	544	24	545	7	545	6	0
56	0.32	0.05486	0.00099	0.61374	0.01162	0.08115	0.00105	406	40	503	6	486	7	−24
57	0.20	0.05856	0.00069	0.75110	0.01008	0.09304	0.00116	551	25	574	7	569	6	−4
58	0.07	0.12529	0.00124	6.48303	0.07756	0.37530	0.00464	2033	17	2054	22	2044	11	−1
59	0.30	0.05870	0.00120	0.70933	0.01493	0.08764	0.00115	556	44	542	7	544	9	3
60	0.25	0.05980	0.00067	0.70553	0.00914	0.08557	0.00106	597	24	529	6	542	5	11
61	0.48	0.05756	0.00063	0.67718	0.00867	0.08533	0.00106	513	24	528	6	525	5	−3
62	0.20	0.05748	0.00072	0.65070	0.00899	0.08214	0.00100	510	27	509	6	509	6	0
63	0.44	0.06318	0.00168	1.02092	0.02727	0.11725	0.00160	714	56	715	9	714	14	0
64	0.28	0.05890	0.00070	0.73858	0.00987	0.09097	0.00110	564	26	561	7	562	6	0
65	0.51	0.05738	0.00069	0.64595	0.00868	0.08168	0.00099	506	26	506	6	506	5	0
66	0.27	0.05618	0.00111	0.57247	0.01163	0.07393	0.00094	459	43	460	6	460	8	0
67	0.19	0.05716	0.00070	0.63175	0.00857	0.08019	0.00097	497	27	497	6	497	5	0
68	0.15	0.05749	0.00148	0.66511	0.01725	0.08393	0.00112	510	56	520	7	518	11	−2
69	0.37	0.05774	0.00087	0.66359	0.01071	0.08339	0.00103	520	33	516	6	517	7	1
70	0.06	0.05786	0.00067	0.64304	0.00837	0.08064	0.00098	524	25	500	6	504	5	5
71	0.32	0.05730	0.00070	0.64885	0.00884	0.08215	0.00100	503	27	509	6	508	5	−1
72	0.20	0.05763	0.00075	0.62901	0.00900	0.07920	0.00097	515	29	491	6	496	6	5
73	0.14	0.10463	0.00118	3.93198	0.05016	0.27267	0.00332	1708	21	1554	17	1620	10	9
AR12: Altai Paragneiss														
1	0.01	0.05724	0.00067	0.63788	0.00807	0.08082	0.00094	500	26	501	6	501	5	0
2	0.20	0.05890	0.00070	0.74086	0.00950	0.09123	0.00107	563	26	563	6	563	6	0
3	0.01	0.05742	0.00084	0.63712	0.00973	0.08048	0.00096	507	32	499	6	501	6	2
4	0.21	0.06910	0.00109	1.43043	0.02336	0.15014	0.00181	902	32	902	10	902	10	0
5	0.49	0.05990	0.00072	0.75188	0.00970	0.09104	0.00106	600	26	562	6	569	6	6
6	0.25	0.06069	0.00075	0.83917	0.01106	0.10028	0.00117	628	26	616	7	619	6	2
7	0.27	0.06142	0.00094	0.89740	0.01422	0.10598	0.00127	654	32	649	7	650	8	1
8	0.27	0.06130	0.00080	0.90780	0.01260	0.10741	0.00126	650	28	658	7	656	7	−1
9	0.26	0.06034	0.00081	0.83324	0.01181	0.10015	0.00118	616	29	615	7	615	7	0
10	0.68	0.05724	0.00104	0.63310	0.01169	0.08022	0.00098	500	39	497	6	498	7	1
11	0.02	0.05441	0.00081	0.46909	0.00725	0.06252	0.00074	388	33	391	5	391	5	−1
12	0.67	0.06724	0.00087	1.40231	0.01936	0.15126	0.00178	845	27	908	10	890	8	−7
13	0.37	0.06959	0.00077	1.46549	0.01767	0.15274	0.00178	916	22	916	10	916	7	0
14	0.26	0.05720	0.00088	0.63552	0.01012	0.08058	0.00096	499	34	500	6	500	6	0
15	0.10	0.06987	0.00225	1.46249	0.04643	0.15181	0.00220	925	65	911	12	915	19	1
16	0.29	0.05917	0.00071	0.76079	0.00987	0.09325	0.00109	574	26	575	6	575	6	0
17	0.10	0.05794	0.00115	0.68353	0.01373	0.08556	0.00105	527	43	529	6	529	8	0
18	0.01	0.05609	0.00082	0.56951	0.00873	0.07364	0.00087	456	32	458	5	458	6	1
19	0.49	0.05784	0.00105	0.66943	0.01234	0.08395	0.00102	523	39	520	6	520	8	1
20	0.45	0.06466	0.00122	1.11898	0.02136	0.12551	0.00155	763	39	762	9	763	10	0
21	0.02	0.05458	0.00087	0.46963	0.00777	0.06241	0.00075	395	35	390	5	391	5	1
22	0.58	0.05810	0.00220	0.68959	0.02562	0.08609	0.00127	533	81	532	8	533	15	0
23	0.18	0.05821	0.00108	0.70282	0.01321	0.08757	0.00107	537	41	541	6	541	8	−1
24	0.21	0.05863	0.00066	0.72380	0.00891	0.08952	0.00104	554	24	553	6	553	5	0
25	0.01	0.05785	0.00062	0.67095	0.00799	0.08411	0.00097	524	24	521	6	521	5	1
26	0.77	0.12593	0.00127	6.47313	0.07320	0.37276	0.00430	2042	18	2042	20	2042	10	0
27	0.01	0.05626	0.00074	0.57488	0.00809	0.07410	0.00087	462	29	461	5	461	5	0
28	0.49	0.05910	0.00065	0.75086	0.00909	0.09214	0.00107	571	24	568	6	569	5	0
29	0.03	0.05655	0.00067	0.59344	0.00764	0.07610	0.00088	473	26	473	5	473	5	0
30	0.01	0.05452	0.00078	0.46789	0.00701	0.06223	0.00073	393	32	389	4	390	5	1
31	0.09	0.05636	0.00086	0.58148	0.00924	0.07481	0.00089	466	34	465	5	465	6	0
32	0.15	0.05920	0.00065	0.77657	0.00938	0.09512	0.00110	575	24	586	6	584	5	−2
33	0.17	0.06617	0.00071	1.22375	0.01456	0.13412	0.00155	812	22	811	9	812	7	0
34	0.38	0.06487	0.00105	1.14156	0.01903	0.12762	0.00153	770	34	774	9	773	9	−1
35	0.17	0.05970	0.00066	0.80208	0.00977	0.09742	0.00113	593	23	599	7	598	6	−1
36	0.26	0.06483	0.00083	1.05963	0.01449	0.11853	0.00139	769	27	722	8	734	7	6
37	0.06	0.05417	0.00106	0.46536	0.00898	0.06171	0.00074	378	43	388	5	386	6	−3
38	0.11	0.06003	0.00072	0.82661	0.01074	0.09986	0.00116	605	26	614	7	612	6	−2
39	0.04	0.05433	0.00085	0.47012	0.00744	0.06189	0.00072	385	35	391	4	387	5	−2
40	0.38	0.05748	0.00063	0.64953	0.00780	0.08194	0.00095	510	24	508	6	508	5	0
41	0.40	0.05784	0.00067	0.67547	0.00884	0.08471	0.00105	524	25	524	6	524	5	0
42	0.41	0.06750	0.00076	1.26349	0.01621	0.13578	0.00168	853	23	821	10	830	7	4
43	0.23	0.05934	0.00076	0.66698	0.00944	0.08153	0.00101	580	28	505	6	519	6	13
44	0.37	0.05736	0.00073	0.64858	0.00909	0.08202	0.00102	505	28	508	6	508	6	−1

Table A1. (continued)

	Ratios							Ages, Ma						
Sample Spot	Th/U	Pb^{207}/Pb^{206}	1σ	Pb^{207}/U^{235}	1σ	Pb^{206}/U^{238}	1σ	Pb^{207}/Pb^{206}	1σ	Pb^{206}/U^{238}	1σ	Pb^{207}/U^{235}	1σ	Disc%
45	0.30	0.05879	0.00067	0.73753	0.00958	0.09100	0.00112	559	25	561	7	561	6	0
46	0.32	0.06866	0.00090	1.40130	0.02012	0.14804	0.00185	889	27	890	10	890	9	0
47	0.52	0.11165	0.00108	4.96413	0.05728	0.32251	0.00395	1826	18	1802	19	1813	10	1
48	0.45	0.05849	0.00075	0.71343	0.01008	0.08848	0.00110	548	28	547	7	547	6	0
49	0.01	0.05634	0.00064	0.57953	0.00748	0.07461	0.00092	465	25	464	6	464	5	0
50	0.03	0.05662	0.00065	0.60125	0.00784	0.07702	0.00095	476	26	478	6	478	5	0
51	0.01	0.05681	0.00064	0.59962	0.00766	0.07656	0.00094	484	25	476	6	477	5	2
52	0.37	0.10445	0.00112	4.32475	0.05327	0.30033	0.00371	1705	20	1693	18	1698	10	1
53	0.21	0.06557	0.00077	1.18138	0.01559	0.13070	0.00162	793	24	792	9	792	7	0
54	0.37	0.05763	0.00086	0.66313	0.01060	0.08346	0.00105	516	33	517	6	517	6	0
55	0.27	0.06614	0.00144	1.22054	0.02708	0.13386	0.00179	811	45	810	10	810	12	0
56	0.37	0.05680	0.00062	0.67429	0.00843	0.08611	0.00106	483	24	533	6	523	5	−10
57	0.49	0.05708	0.00072	0.67114	0.00938	0.08528	0.00106	494	28	528	6	521	6	−7
58	0.07	0.05645	0.00064	0.58760	0.00759	0.07550	0.00093	470	25	469	6	469	5	0

[a]Disc.(%) = (1 − ($^{206}Pb/^{238}U$ age)/($^{207}Pb/^{206}Pb$ age)) × 100.

Table A2. Lu–Hf Data for Zircons From the Chinese Altai Metasedimentary Rocks[a]

Sample	$^{176}Yb/^{177}Hf$	2σ	$^{176}Lu/^{177}Hf$	2σ	$^{176}Hf/^{177}Hf$	2σ	Age, Ma	$(^{176}Hf/^{177}Hf)i$	$\varepsilon_{Hf}(t)$	T^{c}_{DM}	2σ	$f_{Lu/Hf}$
					KK03: Habahe Schist (N47°10′52.7″ E89°46′48.7″)							
1	0.020671	0.000899	0.000571	0.000024	0.281240	0.000038	1994	0.281218	−11	3002	62	−0.98
2	0.033615	0.000352	0.000927	0.000011	0.282114	0.000025	516	0.282105	−12	1864	43	−0.97
3	0.098995	0.003300	0.002161	0.000058	0.282356	0.000026	498	0.282335	−4	1470	43	−0.93
4	0.054874	0.000500	0.001582	0.000014	0.282759	0.000027	527	0.282743	11	752	47	−0.95
5	0.005900	0.000024	0.000192	0.000001	0.281166	0.000030	2453	0.281157	−2	2972	52	−0.99
6	0.020115	0.000139	0.000545	0.000002	0.282413	0.000029	537	0.282408	−1	1335	51	−0.98
7	0.018237	0.001051	0.000509	0.000018	0.282327	0.000026	1475	0.282313	17	1238	44	−0.98
8	0.048439	0.000429	0.001223	0.000012	0.281967	0.000035	527	0.281955	−17	2119	59	−0.96
9	0.028995	0.000448	0.000788	0.000009	0.282595	0.000026	511	0.282588	5	1028	45	−0.98
10	0.021042	0.000170	0.000648	0.000007	0.282454	0.000032	827	0.282444	7	1195	55	−0.98
11	0.026606	0.000168	0.000862	0.000011	0.282550	0.000025	769	0.282537	9	1047	43	−0.97
12	0.024396	0.000102	0.000767	0.000003	0.282447	0.000026	769	0.282436	5	1224	45	−0.98
13	0.027349	0.000595	0.000768	0.000012	0.282123	0.000031	476	0.282116	−13	1854	53	−0.98
14	0.019332	0.001977	0.000578	0.000056	0.281020	0.000025	2721	0.280990	−2	3180	34	−0.98
15	0.018616	0.000160	0.000536	0.000003	0.282280	0.000031	518	0.282275	−6	1571	54	−0.98
16	0.003772	0.000052	0.000094	0.000001	0.281065	0.000031	1820	0.281062	−20	3320	53	−1.00
17	0.025042	0.001396	0.000873	0.000034	0.282456	0.000025	499	0.282448	0	1275	42	−0.97
18	0.027838	0.000546	0.000739	0.000005	0.282267	0.000027	503	0.282260	−7	1600	47	−0.98
19	0.026945	0.000661	0.000788	0.000010	0.282824	0.000029	490	0.282817	12	631	51	−0.98
20	0.023808	0.001089	0.000612	0.000017	0.282221	0.000031	779	0.282212	−3	1612	53	−0.98
21	0.023304	0.000513	0.000656	0.000019	0.282869	0.000024	491	0.282863	14	551	42	−0.98
22	0.019165	0.000325	0.000673	0.000006	0.282368	0.000025	733	0.282359	2	1369	44	−0.98
					KK10: Habahe Migmatite (N47°06′40.9″ E89°49′25.3″)							
1	0.073084	0.001153	0.002187	0.000029	0.282645	0.000017	381	0.282629	3	990	30	−0.93
2	0.074992	0.002868	0.001783	0.000045	0.282390	0.000020	670	0.282367	0	1371	33	−0.95
3	0.015188	0.000101	0.000417	0.000001	0.281954	0.000024	723	0.281948	−13	2083	41	−0.99
4	0.073458	0.002616	0.002106	0.000054	0.282718	0.000033	386	0.282702	6	860	56	−0.94
5	0.082309	0.004951	0.001996	0.000105	0.282586	0.000018	370	0.282572	1	1091	28	−0.94
6	0.033048	0.000194	0.000829	0.000006	0.282428	0.000017	509	0.282420	−1	1321	30	−0.98
7	0.049574	0.000320	0.001328	0.000010	0.282393	0.000028	682	0.282376	1	1353	48	−0.96
8	0.038425	0.000490	0.001140	0.000015	0.282162	0.000019	455	0.282153	−12	1796	31	−0.97
9	0.055810	0.000250	0.001673	0.000019	0.282659	0.000021	391	0.282646	4	957	36	−0.95
10	0.134759	0.001310	0.004159	0.000032	0.282623	0.000028	471	0.282587	4	1040	48	−0.87
11	0.080415	0.002271	0.002740	0.000063	0.282591	0.000025	460	0.282568	3	1076	41	−0.92
12	0.063106	0.001473	0.001834	0.000090	0.282538	0.000018	471	0.282521	2	1154	29	−0.94
13	0.081828	0.003704	0.002648	0.000089	0.282671	0.000026	379	0.282652	4	950	43	−0.92
14	0.053907	0.000884	0.001847	0.000019	0.282410	0.000034	644	0.282388	1	1341	58	−0.94

Table A2. (continued)

Sample	$^{176}Yb/^{177}Hf$	2σ	$^{176}Lu/^{177}Hf$	2σ	$^{176}Hf/^{177}Hf$	2σ	Age, Ma	$(^{176}Hf/^{177}Hf)i$	$\varepsilon_{Hf}(t)$	T^{c}_{DM}	2σ	$f_{Lu/Hf}$
15	0.052980	0.000824	0.001529	0.000054	0.282649	0.000020	385	0.282638	4	973	34	−0.95
16	0.057717	0.000725	0.001476	0.000008	0.282641	0.000021	401	0.282630	4	982	37	−0.96
17	0.090063	0.000638	0.003225	0.000026	0.281994	0.000030	556	0.281961	−16	2101	50	−0.90
18	0.049029	0.000376	0.001499	0.000024	0.282771	0.000024	457	0.282758	10	744	42	−0.95
19	0.050763	0.001398	0.001746	0.000046	0.282298	0.000032	509	0.282282	−6	1561	53	−0.95
20	0.112322	0.005620	0.003770	0.000199	0.282649	0.000032	388	0.282622	3	1001	50	−0.89
21	0.053331	0.000465	0.001868	0.000012	0.282571	0.000022	375	0.282558	1	1115	38	−0.94
BH09: Habahe Siltstone (N48°32′19.6″ E86°42′17.2″)												
1	0.025397	0.000308	0.000914	0.000010	0.282732	0.000016	490	0.282724	9	795	27	−0.97
2	0.026974	0.000310	0.000871	0.000004	0.282355	0.000016	500	0.282347	−4	1450	27	−0.97
3	0.094080	0.000955	0.002280	0.000019	0.282384	0.000020	478	0.282364	−4	1426	34	−0.93
4	0.031694	0.000206	0.000829	0.000004	0.282399	0.000016	476	0.282392	−3	1378	27	−0.98
5	0.032495	0.000148	0.000924	0.000002	0.282821	0.000017	489	0.282813	12	639	30	−0.97
6	0.027525	0.000483	0.000915	0.000013	0.282886	0.000016	524	0.282877	15	517	29	−0.97
7	0.016604	0.000186	0.000409	0.000003	0.280957	0.000019	1962	0.280942	−21	3487	33	−0.99
8	0.029485	0.000338	0.000707	0.000003	0.282839	0.000019	441	0.282833	12	617	33	−0.98
9	0.029116	0.000318	0.000737	0.000002	0.282293	0.000020	494	0.282286	−6	1556	35	−0.98
10	0.019940	0.000572	0.000489	0.000013	0.281181	0.000018	2742	0.281155	4	2883	30	−0.99
11	0.015528	0.000060	0.000527	0.000002	0.282862	0.000020	519	0.282857	14	554	36	−0.98
12	0.001560	0.000109	0.000042	0.000003	0.281105	0.000015	2021	0.281103	−14	3193	25	−1.00
13	0.022665	0.000078	0.000655	0.000005	0.282535	0.000019	854	0.282524	10	1046	34	−0.98
14	0.016144	0.000086	0.000435	0.000001	0.282284	0.000022	465	0.282281	−7	1573	37	−0.99
15	0.040343	0.000158	0.001143	0.000006	0.282861	0.000017	516	0.282850	14	566	31	−0.97
16	0.002403	0.000214	0.000049	0.000004	0.280929	0.000014	1782	0.280927	−26	3561	23	−1.00
17	0.022721	0.000183	0.000661	0.000001	0.282645	0.000021	490	0.282639	6	944	37	−0.98
18	0.043381	0.000342	0.001080	0.000005	0.282409	0.000020	468	0.282399	−3	1367	35	−0.97
19	0.027012	0.000236	0.000662	0.000003	0.282429	0.000018	476	0.282423	−2	1324	32	−0.98
20	0.033862	0.000858	0.000934	0.000022	0.282452	0.000016	469	0.282444	−1	1290	28	−0.97
21	0.018537	0.000437	0.000581	0.000010	0.282806	0.000017	498	0.282801	12	658	30	−0.98
22	0.030629	0.000420	0.000961	0.000009	0.282278	0.000015	480	0.282269	−7	1589	26	−0.97
23	0.036367	0.000319	0.001073	0.000006	0.281688	0.000017	729	0.281673	−23	2552	28	−0.97
24	0.015415	0.000027	0.000409	0.000003	0.282227	0.000016	505	0.282223	−8	1664	27	−0.99
25	0.026690	0.000354	0.001069	0.000013	0.281913	0.000024	816	0.281896	−13	2148	41	−0.97
KK01: Kangbutiebao Mylonite (N46°59′48.7″ E89°44′41.6″)												
1	0.041989	0.000405	0.001268	0.000009	0.282669	0.000016	520	0.282657	7	905	27	−0.96
2	0.025808	0.000171	0.000761	0.000006	0.282430	0.000017	509	0.282422	−1	1316	30	−0.98
3	0.018194	0.000379	0.000612	0.000017	0.281855	0.000018	1708	0.281835	5	2010	30	−0.98
4	0.039467	0.000314	0.001304	0.000012	0.282779	0.000016	500	0.282767	11	716	27	−0.96
5	0.022228	0.000292	0.000606	0.000002	0.282377	0.000016	516	0.282371	−3	1404	28	−0.98
6	0.018160	0.000100	0.000517	0.000002	0.282434	0.000018	491	0.282429	−1	1310	30	−0.98
7	0.053371	0.001165	0.001653	0.000022	0.282904	0.000019	520	0.282888	16	498	33	−0.95
8	0.073163	0.001213	0.001906	0.000043	0.282335	0.000019	506	0.282316	−5	1501	31	−0.94
9	0.043192	0.000561	0.001100	0.000003	0.282428	0.000016	561	0.282416	0	1314	27	−0.97
10	0.012100	0.000070	0.000378	0.000003	0.282112	0.000019	715	0.282107	−8	1810	33	−0.99
11	0.057106	0.000419	0.001236	0.000006	0.282400	0.000021	528	0.282388	−2	1371	35	−0.96
12	0.059357	0.001510	0.001813	0.000041	0.282622	0.000022	509	0.282604	5	1000	36	−0.95
13	0.069041	0.000535	0.001550	0.000004	0.282575	0.000028	503	0.282560	4	1078	49	−0.95
14	0.041598	0.000262	0.001072	0.000016	0.282824	0.000020	542	0.282813	13	625	35	−0.97
15	0.041594	0.000443	0.001129	0.000007	0.281033	0.000020	2033	0.280990	−18	3385	34	−0.97
16	0.017402	0.000285	0.000467	0.000002	0.282344	0.000017	574	0.282339	−3	1445	30	−0.99
17	0.087233	0.000682	0.002073	0.000005	0.282823	0.000024	492	0.282804	12	654	42	−0.94
18	0.055752	0.000943	0.001318	0.000008	0.282519	0.000020	545	0.282505	3	1163	35	−0.96
19	0.022035	0.000237	0.000559	0.000001	0.282487	0.000027	444	0.282482	0	1229	47	−0.98
20	0.065868	0.000572	0.001841	0.000015	0.282720	0.000027	493	0.282703	8	831	46	−0.94
21	0.072692	0.000621	0.001829	0.000005	0.282663	0.000020	526	0.282645	7	924	35	−0.94
22	0.024718	0.000401	0.000610	0.000003	0.282428	0.000019	588	0.282421	1	1298	32	−0.98
23	0.056273	0.000973	0.001313	0.000006	0.282707	0.000021	476	0.282695	8	850	37	−0.96
24	0.052996	0.001064	0.001418	0.000013	0.282648	0.000021	501	0.282635	6	949	36	−0.96
25	0.044593	0.000907	0.001210	0.000023	0.282508	0.000016	420	0.282498	0	1207	28	−0.96
26	0.037997	0.000272	0.001304	0.000011	0.282843	0.000019	530	0.282830	14	598	33	−0.96
27	0.018049	0.000143	0.000458	0.000003	0.282408	0.000018	532	0.282403	−1	1344	32	−0.99
28	0.026063	0.000395	0.000684	0.000003	0.282426	0.000013	599	0.282418	1	1300	22	−0.98
29	0.065662	0.000707	0.001702	0.000007	0.282644	0.000019	457	0.282630	5	969	33	−0.95
AR12: Altai Paragneiss (N47°34′53.7″ E88°25′11.3″)												
1	0.029791	0.001015	0.000936	0.000033	0.282315	0.000023	533	0.282306	−5	1513	39	−0.97
2	0.020162	0.000613	0.000643	0.000021	0.282409	0.000020	828	0.282399	5	1274	35	−0.98

Table A2. (continued)

Sample	$^{176}Yb/^{177}Hf$	2σ	$^{176}Lu/^{177}Hf$	2σ	$^{176}Hf/^{177}Hf$	2σ	Age, Ma	$(^{176}Hf/^{177}Hf)i$	$\varepsilon_{Hf}(t)$	T^{c}_{DM}	2σ	$f_{Lu/Hf}$
3	0.027897	0.000617	0.000986	0.000031	0.282591	0.000034	517	0.282581	5	1038	59	−0.97
4	0.005432	0.000430	0.000148	0.000015	0.282647	0.000030	403	0.282645	4	955	51	−1.00
5	0.024100	0.000128	0.000765	0.000005	0.281219	0.000021	2640	0.281181	3	2871	37	−0.98
6	0.034870	0.001164	0.001302	0.000045	0.282511	0.000020	464	0.282499	1	1194	34	−0.96
7	0.031320	0.000264	0.000993	0.000014	0.282347	0.000027	547	0.282337	−3	1455	46	−0.97
8	0.039430	0.000683	0.001395	0.000018	0.282584	0.000022	703	0.282566	8	1015	37	−0.96
9	0.017232	0.001132	0.000626	0.000042	0.282598	0.000024	820	0.282588	12	943	40	−0.98
10	0.036581	0.000552	0.001137	0.000016	0.282574	0.000022	561	0.282562	5	1059	39	−0.97
11	0.043906	0.002279	0.001605	0.000066	0.282542	0.000027	821	0.282517	9	1068	43	−0.95
12	0.032603	0.000377	0.001196	0.000015	0.282312	0.000024	524	0.282300	−5	1525	40	−0.96
13	0.039662	0.000550	0.001261	0.000018	0.282391	0.000023	1190	0.282363	12	1235	39	−0.96
14	0.022394	0.002127	0.000814	0.000083	0.282690	0.000039	444	0.282684	7	878	65	−0.98
15	0.035315	0.000493	0.001243	0.000023	0.282568	0.000023	391	0.282559	1	1110	39	−0.96
16	0.055509	0.003272	0.001887	0.000103	0.282380	0.000031	508	0.282362	−3	1422	51	−0.94
17	0.033060	0.001329	0.001249	0.000051	0.282391	0.000033	774	0.282373	3	1334	55	−0.96
18	0.043947	0.001937	0.001367	0.000045	0.282509	0.000023	916	0.282486	10	1097	37	−0.96
19	0.015345	0.000575	0.000541	0.000020	0.282654	0.000034	410	0.282650	5	946	59	−0.98
20	0.033020	0.000712	0.001030	0.000027	0.282296	0.000026	884	0.282279	2	1468	43	−0.97
21	0.055528	0.001139	0.001714	0.000067	0.282697	0.000029	490	0.282681	8	871	49	−0.95
22	0.038983	0.000994	0.001283	0.000029	0.282683	0.000027	391	0.282673	5	910	46	−0.96
23	0.034634	0.001072	0.001142	0.000038	0.282608	0.000023	497	0.282597	5	1015	38	−0.97
24	0.032566	0.000175	0.001060	0.000004	0.282087	0.000042	911	0.282069	−5	1826	72	−0.97

[a]$T^{c}_{DM} = t + (1/\lambda) \times \ln[1 + ((^{176}Hf/^{177}Hf)_{S,t} - (^{176}Hf/^{177}Hf)_{DM,t})/((^{176}Lu/^{177}Hf)_{UC} - (^{176}Lu/^{177}Hf)_{DM})]$, where UC, S and DM are the upper continental crust, the sample and the depleted mantle, respectively. The $^{206}Pb/^{238}U$ ages are used for zircons younger than 1000 Ma, and $^{207}Pb/^{206}Pb$ ages are used for zircons older than 1000 Ma.

the sedimentary provenance. Therefore our Hf isotopic data are also consistent with the above tectonic interpretation.

7. Conclusions

[36] On the basis of our U–Pb and Hf isotope data for the detrital zircons from the metasedimentary rocks of the Chinese Altai, we have the following major conclusions.

[37] 1. The Habahe Group was deposited in the Middle Ordovician or later, not in the Precambrian. The deposition age of the Kangbutiebao Formation was later than the Early Silurian, which is consistent with the upper Silurian to lower Devonian age assigned to this formation.

[38] 2. The migmatite from the Habahe Group and the garnet-sillimanite gneiss from the Altai Formation both underwent strong metamorphism in the Devonian. Together with the published Permian metamorphic ages, these metamorphic events show a multiple thermal history for the Chinese Altai.

[39] 3. The provenance of the metasedimentary rocks in the Chinese Altai orogen was dominated by Cambrian to Early Ordovician igneous rocks, with subordinate Neoproterozoic and minor Paleoproterozoic and Archean crustal materials.

[40] 4. The Early Paleozoic and Neoproterozoic were important accretionary periods for the Chinese Altai, during which large volumes of juvenile materials were added to the crust.

[41] 5. The Chinese Altai was an active, not passive, continental margin in the Early Paleozoic, which is inconsistent with a Precambrian microcontinent model and reveals an arc accretionary history.

Appendix A

[42] Here we provide detailed U-Pb and Lu-Hf data for zircons from the Chinese Altai metasedimentary rocks, in Tables A1 and A2.

[43] **Acknowledgments.** We thank Onno Oncken, Paul Robinson, and another anonymous reviewer for their constructive suggestions and useful instructions. We are very grateful to Paul Robinson for his polishing work which substantially improved the manuscript. This study was supported by research grants from National Basic Research Program of China (2007CB411308), Hong Kong Research Grant Council (HKU7040/04P), and NSFC (40421303, 40572043). We thank Liewen Xie, Yueheng Yang, Linli Chen, Buyun Wang, Jean Wong, Yanhong He, and Hongyan Geng for laboratory assistance.

References

Andersen, T. (2005), Detrital zircons as tracers of sedimentary provenance: Limiting conditions from statistics and numerical simulation, *Chem. Geol.*, *216*, 270–294.

Andersen, T., K. Laajoki, and A. Saeed (2004), Age, provenance and tectonostratigraphic status of the Mesoproterozoic Blefjell quartzite, Telemark sector, southern Norway, *Precambrian Res.*, *135*, 217–244.

Badarch, G., W. D. Cunningham, and B. F. Windley (2002), A new terrane subdivision for Mongolia: Implications for the Phanerozoic crustal growth of central Asia, *J. Asian Earth Sci.*, *21*, 87–110.

Berzin, N. A., and N. L. Dobretsov (Eds.) (1993), Geodynamic evolution of southern Siberia in Late Precambrian–early Paleozoic time, in *Reconstruction of the Paleosian Ocean*, pp. 45–62, VSP Inter. Sci., Utrecht, Netherlands.

Bibikova, E. V., T. V. Grachova, V. A. Makarov, and K. B. Seslavinsky (1981), The oldest metamorphic rocks of the north–east of the USSR (U-Pb method of dating), in *Geology and Metallogeny of Precambrian of Far East*, edited by K. O. Krats and E. A. Kulish, pp. 46–55, Nauka, Leningrad, Russia.

Bingen, B., A. Birkeland, A. Nordgulen, and E. M. O. Sigmond (2001), Correlation of supracrustal sequences and origin of terranes in the Sveconorwegian orogen of SW Scandinavia: SIMS data on zircon in clastic metasediments, *Precambrian Res.*, *108*, 293–318.

Blichert-Toft, J., and F. Albarede (1997), The Lu-Hf geochemistry of the chondrites and the evolution of the mantle–crust system, *Earth Planet. Sci. Lett.*, *148*, 243–258.

Bruguier, O. (1996), U-Pb ages on single detrital zircon grains from the Tasmiyele Group: Implications for the evolution of the Olekma Block (Aldan Shield, Siberia), *Precambrian Res.*, *78*, 197–210.

Bureau of Geology and Mineral Resources of Xinjiang Uygur Autonomous Region (BGMRX) (Eds.) (1993), *Regional Geology of Xinjiang Uygur Autonomous Region, People's Republic of China, Ministry of Geology and Mineral Resources*, *Geol. Mem.*, Ser. 1, vol. 32, pp. 6–206, Geol. Publ. House, Beijing.

Chang, E. Z., R. G. Coleman, and D. X. Ying (1995), *Tectonic Transect Map Across Russia-Mongolia-China*, Stanford Univ. Press, Stanford, Calif.

Chen, B., and B. M. Jahn (2002), Geochemical and isotopic studies of the sedimentary and granitic rocks of the Altai orogen of NW China and their tectonic implications, *Geol. Mag.*, *139*(1), 1–13.

Chen, B., and B. M. Jahn (2004), Genesis of post-collisional granitoids and basement nature of the Junggar Terrane, NW China: Nd–Sr isotope and trace element evidence, *J. Asian Earth. Sci.*, *23*, 691–703.

Chen, H. L., S. F. Yang, Z. L. Li, X. Yu, W. J. Xiao, C. Yuan, X. B. Lin, and J. L. Li (2006), Zircon SHRIMP U-Pb chronology of Fuyun basic granulite and its tectonic significance in Altaid orogenic belt, *Acta Petrol. Sin.*, *22*, 1351–1358.

Chen, Y. C., , Q. T. Ye, J. B. Wang, and X. J. Rui (Eds.) (2003), *Geology of Ore Deposits, Metallogenic Regularity and Technoenocomic Evaluation on the Altay Metallogenic Belt, Xinjiang Area, China*, pp. 1–43, Geol. Publ. House, Beijing.

Chen, Z. F., S. D. Cheng, and Y. H. Liang (Eds.) (1997), *Opening-Closing Tectonics and Mineralization*, pp. 10–90, Sci. and Technol. and Sanit. Press, Urumchi, China.

Chiaradia, M., D. Konopelko, R. Seltmann, and R. A. Cliff (2006), Lead isotope variations across terrane boundaries of the Tien Shan and Chinese Altay, *Miner. Deposita*, *41*, 411–428.

Coleman, R. G. (1989), Continental growth of northwest China, *Tectonics*, *8*, 621–635.

Corfu, F., J. M. Hanchar, P. W. Hoskin, and P. Kinny (2003), Atlas of zircon textures, *Rev. Miner. Geochem.*, *53*, 468–500.

Darby, B. J., and G. Gehrels (2006), Detrital zircon reference for the North China block, *J. Asian Earth Sci.*, *26*, 637–648.

Dobretsov, N. L., N. A. Berzin, and M. M. Buslov (1995), Opening and the tectonic evolution of Paleo-Asian ocean, *Int. Geol. Rev.*, *35*, 335–360.

Dobretsov, N. L., M. M. Buslov, and U. Yu (2004), Fragments of oceanic islands in accretion-collision areas of Gorny Altai and Salair, southern Siberia, Russia: Early stages of continental crustal growth of the Siberian continent in Vendian–Early Cambrian time, *J. Asian Earth Sci.*, *23*, 673–690.

Ermolov, P. V. (1984), Fold system and metamorphic complex in Aletai mineral district and some geological structure characteristics, *Geol. Struct.*, *4*, 61–71.

Federovskii, V. S., E. V. Khain, A. G. Vladimirov, S. A. Karkopolov, A. S. Gibsher, and A. E. Izokh (1995), Tectonics, metamorphism, and magmatism of collisional zones of the Central Asian Caledonides, *Geotectonics*, *29*, 193–212.

Fedo, C. M., K. N. Sircombe, and R. H. Rainbird (2003), Detrital zircon analysis of the sedimentary record, *Rev. Miner. Geochem.*, *53*, 277–303.

Frost, B. R., O. V. Avchenko, K. R. Chamberlain, and C. D. Frost (1998), Evidence for extensive Proterozoic remobilization of the Aldan shield and implications for Proterozoic plate tectonic reconstructions of Siberia and Laurentia, *Precambrian Res.*, *89*, 1–23.

Gladkochub, D. P., M. T. D. Wingate, S. A. Pisarevsky, T. V. Donskaya, A. M. Mazukabzov, V. A. Ponomarchuk, and A. M. Stanevich (2006), Mafic intrusions in southwestern Siberia and implications for a Neoproterozoic connection with Laurentia, *Precambrian Res.*, *147*, 260–278.

Griffin, W. L., E. A. Belousova, S. R. Shee, N. J. Pearson, and S. Y. O'Reilly (2004), Archaean crustal evolution in the northern Yilgarn Craton: U-Pb and Hf isotope evidence from detrital zircons, *Precambrian Res.*, *131*, 231–282.

Group for Compilation of Regional Stratigraphy of Xinjiang (GCRSX) (Eds.) (1981), *Regional Stratigraphic Table of NW China: Xinjiang Uygur Autonomous Region Fascicule*, pp. 7–11, Geol. Publ. House, Beijing.

Guan, H., M. Sun, S. A. Wilde, X. H. Zhou, and M. G. Zhai (2002), SHRIMP U-Pb zircon geochronology of the Fuping Complex: Implications for formation and assembly of the North China craton, *Precambrian Res.*, *113*, 1–18.

Guo, S. J., Z. C. Zhang, S. W. Liu, and H. M. Li (2003), U-Pb geochronological evidence for the early Precambrian complex of the Tarim Craton, NW China, *Acta Petrol. Sin.*, *19*, 537–542.

Han, B. F., and G. Q. He (1991), The tectonic nature of the Devonian volcanic belt on the southern edge of Altay Mountains in China, *Geosci. Xinjiang*, *3*, 89–100.

Han, B. F., S. G. Wang, B. M. Jahn, D. W. Hong, H. Kagami, and Y. L. Sun (1997), Depleted-mantle source for the Ulungur River A-type granites from North Xinjiang, China: Geochemistry and Nd-Sr isotopic evidence, and implications for Phanerozoic crustal growth, *Chem. Geol.*, *138*, 135–159.

Hanchar, J. M., and R. L. Rundnick (1995), Revealing hidden structures: The application of cathodoluminescene and back-scattered electron imaging to dating zircons from lower crustal xenoliths, *Lithos*, *36*, 289–303.

He, G. Q., B. F. Han, Y. J. Yue, and J. H. Wang (1990), Tectonic division and crustal evolution of Altay orogenic belt in China, *Geosci. Xinjiang*, *2*, 9–20.

Helo, C., E. Hegner, A. Kröner, G. Badarch, O. Tomurtogoo, B. F. Windley, and P. Dulski (2006), Geochemical signature of Paleozoic accretionary complexes of the Central Asian Orogenic Belt in South Mongolia: Constraints on arc environments and crustal growth, *Chem. Geol.*, *227*, 236–257.

Hong, D. W., J. S. Zhang, T. Wang, S. G. Wang, and X. L. Xie (2004), Continental crustal growth and the supercontinental cycle: Evidence from the Central Asian Orogenic Belt, *J. Asian Earth Sci.*, *23*, 799–813.

Hoskin, P. W. O., and L. P. Black (2000), Metamorphic zircon formation by solid-state recrystallization of protolith igneous zircons, *J. Metamorph. Geol.*, *18*, 423–439.

Hu, A. Q., and G. J. Wei (2003), A review of ages of basement rocks from Junggar basin in Xinjiang, China—Based on studies of geochronology, *Xinjiang Geol.*, *21*, 389–406.

Hu, A. Q., and G. J. Wei (2006), On the age of the Neo-Archean Qingir gray gneisses from the northern Tarim basin, Xinjiang, China, *Acta Geol. Sin.*, *80*, 126–134.

Hu, A. Q., B. M. Jahn, G. Zhang, Y. Chen, and Q. Zhang (2000), Crustal evolution and Phanerozoic crustal growth in northern Xinjiang: Nd isotope evidence. 1. Isotopic characterization of basement rocks, *Tectonophysics*, *328*, 15–51.

Hu, A. Q., G. X. Zhang, Q. F. Zhang, T. D. Li, and J. B. Zhang (2002), A review on ages of Precambrian metamorphic rocks from Altai orogen in Xinjiang, NW China, *Chin. J. Geol.*, *37*, 129–142.

Hu, A. Q., G. J. Wei, W. F. Deng, and L. L. Chen (2006), SHRIMP zircon U-Pb dating and its significance for gneisses from the southwest area to Qinghe County in the Altai, China, *Acta Petrol. Sin.*, *22*, 1–10.

Huang, J. Q., C. F. Jiang, and Z. X. Wang (1990), On the opening-closing tectonics and accordion movement of plate in Xiangjiang and adjacent regions (in Chinese), *Geosci. Xinjiang*, *1*, 3–16.

Iizuka, T., and T. Hirata (2005), Improvements of precision and accuracy in in-situ Hf isotope microanalysis of zircon using the laser ablation-MC-ICPMS technique, *Chem. Geol.*, *220*, 121–137.

Jahn, B. M. (2004), The Central Asian Orogenic Belt and growth of the continental crust in the Phanerozoic, in *Aspects of the Tectonic Evolution of China*, edited by J. Malpas et al., *Geol. Soc. Spec. Publ.*, *226*, 73–100.

Jahn, B. M., G. Gruau, R. Capdevila, J. Cornichet, A. Nemchin, R. Pidgeon, and V. A. Rudnik (1998), Archean crustal evolution of the Aldan Shield, Siberia: Geochemical and isotopic constraints, *Precambrian Res.*, *91*, 333–363.

Jahn, B. M., F. Wu, and B. Chen (2000), Granitoids of the Central Asian orogenic belt and continental growth in the Phanerozoic, *Trans. R. Soc. Edinburgh Earth Sci.*, *91*, 181–193.

Khain, E. V., E. V. Bibikova, E. B. Salnikova, A. Kröner, A. S. Gibsher, A. N. Didenko, K. E. Degtyarev, and A. A. Fedotova (2003), The Palaeo-Asian ocean in the Neoproterozoic and early Palaeozoic: New geochronologic data and palaeotectonic reconstructions, *Precambrian Res.*, *122*, 329–358.

Khudoley, A. K., R. H. Rainbird, R. A. Stern, A. P. Kropachev, L. M. Heaman, A. M. Zanin, V. N. Podkovyrov, V. N. Belova, and V. I. Sukhorukov (2001), Sedimentary evolution of the Riphean-Vendian basin of southeastern Siberia, *Precambrian Res.*, *111*, 129–163.

Kröner, A., S. A. Wilde, J. H. Li, and K. Y. Wang (2005), Age and evolution of a late Archean to Paleoproterozoic upper to lower crustal section in the Wutaishan-Hengshan-Fuping terrain of northern China, *J. Asian Earth Sci.*, *24*, 577–595.

Kuzmichev, A., A. Kröner, E. Hegner, D. Y. Liu, and Y. S. Wan (2005), The Shishkhid ophiolite, northern Mongolia: A key to the reconstruction of a Neoproterozoic island-arc system in central Asia, *Precambrian Res.*, *138*, 125–150.

Kuzmichev, A. B., E. V. Bibikova, and D. Z. Zhuravlev (2001), Neoproterozoic (800 Ma) orogeny in the Tuva-Mongolian Massif (Siberia): Island arc-continent collision at the northeast Rodinia margin, *Precambrian Res.*, *110*, 109–126.

Kuzmin, V. V., A. P. Chukhonin, and I. K. Shulezhko (1995), Stages of metamorphic evolution of rocks of crystalline basement of the Kukhtui Uplift (Okhotsk Massif), *Dokl. Russ. Acad. Sci.*, *142*, 789–791.

Li, C. Y., Q. Wang, X. Y. Liu, and Y. Q. Tang (Eds.) (1982), *Explanatory Notes to the Tectonic Map of Asian*, pp. 1–40, Geol. Publ. House, Beijing.

Li, H. J., G. Q. He, T. R. Wu, and B. Wu (2006), Confirmation of Altai-Mongolia microcontinent and its implications, *Acta Petrol. Sin.*, *22*, 1369–1379.

Li, J. Y. (1991), Evolution of Paleozoic plate tectonics of east Junggar, Xinjiang, China, in *Tectonic Evolution of the Southern Margin of the Paleo-Asian Composite Megasuture*, edited by X. C. Xiao and Y. Q. Tang, pp. 92–108, Beijing Sci. and Tech. Publ. House, Beijing.

Li, J., W. Xiao, K. Wang, G. Sun, and L. Gao (2003), Tectonic and metallogenic evolution of the Altay Shan, Northern Xinjiang Uygur Autonomous Region, northwestern China, in *Tectonic Evolution and Metallogeny of the Chinese Altay and Tianshan*, edited by J. Mao et al., pp. 31–74, Cent. for Russ. and Central EurAsian Miner. Stud. (CERCAMS), Beijing.

Li, T. D., and B. H. Poliyangsiji (2001), Tectonics and crustal evolution of Altai in China and Kazakhstan, *Xinjiang Geol.*, *19*, 27–32.

Li, T. D., Z. M. Qi, S. L. Xiao, and B. Q. Wu (1996), New improvement of comparative study of geology and mineralization of Altai between China and Kazakhstan, in *Thesis Volume of the Symposium of the 8th Five Year Plan of Geoscience for*

Contribution to 30th IGC, pp. 256–259, edited by Chinese Geological Society, Metal. Ind. Publ. House, Beijing.

Liu, D. Q., Y. L. Tang, and R. H. Zhou (1998), On basic continental crust of the pre-Sinian of Xinjiang, *Xinjiang Geol.*, *16*, 195–202.

Long, X. P., M. Sun, C. Yuan, W. J. Xiao, H. L. Chen, Y. J. Zhao, K. D. Cai, and J. L. Li (2006), Genesis of carboniferous volcanic rocks in the eastern Junggar: Constraints on the closure of the Junggar Ocean, *Acta Petrol. Sin.*, *22*, 31–40.

Lu, X. P., F. Y. Wu, J. H. Guo, S. A. Wilde, J. H. Yang, X. M. Liu, and X. O. Zhang (2006), Zircon U–Pb geochronological constraints on the Paleoproterozoic crustal evolution of the Eastern block in the North China Craton, *Precambrian Res.*, *146*, 138–164.

Ludwig, K. R. (2003), User's Manual for Isoplot 3.00: A Geochronological Toolkit for Microsoft Excel, *Spec. Publ. 4a*, Berkeley Geochronol. Cent., Berkeley, Calif.

Luo, Y., M. Sun, G. C. Zhao, S. Z. Li, P. Xu, K. Ye, and X. P. Xia (2004), LA-ICP-MS U–Pb zircon ages of the Liaohe Group in the Eastern Block of the North China Craton: Constraints on the evolution of the Jiao-Liao-Ji Belt, *Precambrian Res.*, *134*, 349–371.

McLennan, S. M., B. Bock, W. Compston, S. R. Hemming, and D. K. McDaniel (2001), Detrital zircon geochronology of Taconian and Acadian foreland sedimentary rocks in New England, *J. Sediment. Res.*, *71*, 305–317.

Moecher, D. P., and S. D. Samson (2006), Differential zircon fertility of source terranes and natural bias in the detrital zircon record: Implications for sedimentary provenance analysis, *Earth Planet. Sci. Lett.*, *247*, 252–266.

Nelson, D. R. (2001), An assessment of the determination of depositional ages for Precambrian clastic sedimentary rocks by U-Pb dating of detrital zircon, *Sediment. Geol.*, *141–142*, 37–60.

Payne, J. L., K. M. Barovich, and M. Hand (2006), Provenance of metasedimentary rocks in the northern Gawler Craton, Australia: Implications for Palaeoproterozoic reconstructions, *Precambrian Res.*, *148*, 275–291.

Peng, C. E. (1989), Discovery and geological significance of micropaleoflora fro the Habahe Group in Baikaba district of Xinjiang, *Xinjiang Geol.*, *7*, 19–22.

Rainbird, R. H., R. A. Stern, A. K. Khudoley, A. P. Kropachev, L. M. Heaman, and V. I. Sukhorukov (1998), U–Pb geochronology of Riphean sandstone and gabbro from southeast Siberia and its bearing on the Laurentia-Siberia connection, *Earth Planet. Sci. Lett.*, *164*, 409–420.

Ren, J. S., Z. X. Wang, B. W. Chen, C. F. Jiang, B. G. Niu, J. Y. Li, G. L. Xie, Z. J. He, and Z. G. Liu (Eds.) (1999), *The Tectonic Map of China and Adjacent Regions*, pp. 1–50, Geol. Publ. House, Beijing.

Ross, G. M., and M. E. Villeneuve (1998), Provenance of the Belt Purcell Supergroup, southern British Columbia: A SHRIMP study of detrital zircons, in *Slave-Northern Cordillera Lithoprobe Evolution (SNORCLE) and Cordilleran Tectonics Workshop Meeting Lithoprobe Report 64*, edited by F. A. Cook and P. Erdmer, pp. 186–191, Univ. of Calgary, Calgary, Alberta, Canada.

Salnikova, E. B., I. K. Kozakov, A. B. Kotov, A. Kröner, W. Todt, E. V. Bibikova, A. Nutman, S. Z. Yakovleva, and V. P. Kovach (2001), Age of Palaeozoic granites and metamorphism in the Tuvino-Mongolian Massif of the Central Asian Mobile Belt: Loss of a Precambrian microcontinent, *Precambrian Res.*, *110*, 143–164.

Scherer, E., C. Munker, and K. Mezger (2001), Calibration of the Lutetium-Hafnium clock, *Science*, *293*, 683–687.

Sengör, A. M. C., and B. A. Natal'in (1996), Paleotectonics of Asia: Fragments of a synthesis, in *The Tectonic Evolution of Asia*, pp. 486–640, edited by A. Yin and M. Harrison, Cambridge Univ. Press, Cambridge, U. K.

Sengör, A. M. C., B. A. Natal'in, and V. S. Burtman (1993), Evolution of the Altaid tectonic collage and Paleozoic crustal growth in Asia, *Nature*, *364*, 299–307.

Shan, Q., H. C. Niu, X. Y. Yu, and H. X. Zhang (2005), Geochemistry and zircon U-Pb age of volcanic rocks from the Hanasi basin in the northern Xinjiang and their tectonic significance, *Geochimica*, *34*, 315–327.

Sun, M., C. Yuan, W. Xiao, X. Long, X. Xia, C. Han, and S. Lin (2006), Granitic gneisses and gneissic granites from the Central Terrane of the Chinese Altai Orogen: Zircon ages and tectonic significance, *Eos Trans. AGU*, *87*(36), West. Pac. Geophys. Meet. Suppl., Abstract V25A–06.

Taylor, S. R., and S. M. McLennan (1985), *The Continental Crust, its Composition and Evolution*, pp. 312, Blackwell, Oxford, U. K.

Vernikovskaya, A. E., V. A. Vernikovsky, E. B. Sal'nikova, V. M. Datsenko, A. B. Kotov, V. P. Kovach, A. V. Travin, and S. Z. Yakovleva (2002), Yeruda and Cherimba granitoids (Yenisey Ridge) as indicators of Neoproterozoic collisions, *Russ. Geol. Geophys.*, *43*, 245–259.

Vernikovsky, V. A., A. E. Vernikovskaya, E. B. Sal'nikova, A. B. Kotov, and V. P. Kovach (2002), Postcollision granitoid magmatism in the Transangara region of the Yenisey Ridge: An event 750–720 Ma, *Dokl. Akad. Sci. USSR, Earth Sci. Ser.*, *384*, 362–366.

Vernikovsky, V. A., A. E. Vernikovskaya, A. B. Kotovb, E. B. Sal'nikovab, and V. P. Kovach (2003), Neoproterozoic accretionary and collisional events on the western margin of the Siberian craton: New geological and geochronological evidence from the Yenisey Ridge, *Tectonophysics*, *375*, 147–168.

Wan, Y. S., S. A. Wilde, D. Y. Liu, C. X. Yang, B. Song, and X. Y. Yin (2006), Further evidence for ~1.85 Ga metamorphism in the Central Zone of the North China Craton: SHRIMP U-Pb dating of zircon from metamorphic rocks in the Lushan area, Henan Province, *Gondwana Res.*, *9*, 189–197.

Wang, D. H., Y. C. Chen, Z. G. Xu, T. D. Li, and X. J. Fu (Eds.) (2002), *The Metallogenetic Series and Regularities of Altay Metallogenetic Province*, pp. 412–453, Atom. Energy Publ. House, Beijing.

Wang, F. Z., M. Z. Yang, and J. P. Zheng (2002), Geochemical evidence of the basement assembled by island arc volcanic terranes in Junggar basin, *Acta Pet. Miner.*, *21*(1), 1–10.

Wang, G. Y. (1983), The discovery of Sinian strata in Xinjiang Altay and its significance, *Reg. Geol. China*, *10*, 117–119.

Wang, T., D. W. Hong, B. M. Jahn, Y. Tong, Y. B. Wang, B. F. Han, and X. X. Wang (2006), Timing, petrogenesis, and setting of Paleozoic synorogenic intrusions from the Altai Mountains, northwest China: Implications for the tectonic evolution of an accretionary orogen, *J. Geol.*, *114*, 735–751.

Wang, Z., S. Sun, J. Li, Q. Hou, K. Qin, W. Xiao, and J. Hao (2003), Paleozoic tectonic evolution of the northern Xinjiang, China: Geochemical and geochronological constraints from the ophiolites, *Tectonics*, *22*(2), 1014, doi:10.1029/2002TC001396.

Wilde, S. A., and G. C. Zhao (2005), Archean to Paleoproterozoic evolution of the North China Craton, *J. Asian Earth Sci.*, *24*, 519–522.

Wilde, S. A., X. Z. Zhang, and F. Y. Wu (2000), Extension of a newly identified 500 Ma metamorphic terrane in North East China: Further U-Pb SHRIMP dating of the Mashan Complex, Heilongjiang Province, China, *Tectonophysics*, *328*, 115–130.

Wilde, S. A., F. Y. Wu, and X. Z. Zhang (2003), Late Pan-African magmatism in northeastern China: SHRIMP U-Pb zircon evidence from granitoids in the Jiamusi Massif, *Precambrian Res.*, *122*, 311–327.

Williams, I. S. (2001), Response of detrital zircon and monazite, and their U–Pb isotopic systems, to regional metamorphism and host-rock partial melting, Cooma Complex, southeastern Australia, *Aust. J. Earth Sci.*, *48*, 557–580.

Windley, B. F., A. Kröner, J. Guo, G. Qu, Y. Li, and C. Zhang (2002), Neoproterozoic to Paleozoic geology of the Altai orogen, NW China: New zircon age data and tectonic evolution, *J. Geol.*, *110*, 719–739.

Wu, F. Y., Y. H. Yang, L. W. Xie, J. H. Yang, and P. Xu (2006), Hf isotopic compositions of the standard zircons and baddeleyites used in U-Pb geochronology, *Chem. Geol.*, *234*, 105–126.

Xia, X. P., M. Sun, G. C. Zhao, H. M. Li, and M. F. Zhou (2004), Spot zircon U-Pb isotope analysis by ICP-MS coupled with a frequency quintupled (213 nm) Nd-YAG laser system, *Geochem. J.*, *38*, 191–200.

Xia, X. P., M. Sun, G. C. Zhao, and Y. Luo (2006a), LA-ICP-MS U-Pb geochronology of detrital zircons from the Jining Complex, North China Craton and its tectonic significance, *Precambrian Res.*, *144*, 199–212.

Xia, X. P., M. Sun, G. C. Zhao, F. Y. Wu, P. Xu, J. H. Zhang, and Y. Luo (2006b), U-Pb and Hf isotopic study of detrital zircons from the Wulashan khondalites: Constraints on the evolution of the Ordos Terrane, Western Block of the North China Craton, *Earth Planet. Sci. Lett.*, *241*, 581–593.

Xiao, W. J., B. F. Windley, J. Hao, and M. G. Zhai (2003), Accretion leading to collision and the Permian Solonker suture, Inner Mongolia, China: Termination of the central Asian orogenic belt, *Tectonics*, *22*(6), 1069, doi:10.1029/2002TC001484.

Xiao, W. J., B. F. Windley, G. Badararch, S. Sun, J. Li, K. Qin, and Z. Wang (2004), Paleozoic accretionary and convergent tectonics of the southern Altaids: Implications for the growth of central Asia, *J. Geol. Soc.*, *161*, 1–4.

Xiao, W. J., B. F. Windley, Q. R. Yan, K. Z. Qin, H. L. Chen, C. Yuan, M. Sun, and J. L. Li (2006), SHRIMP zircon age of the Aermantai Ophiolite in the north Xinjiang area, China and its tectonic implications, *Acta Geol. Sin.*, *80*, 32–37.

Xiao, X. C., Y. Q. Tang, J. Y. Li, M. Zhao, Y. M. Feng, and B. Q. Zhu (1990), On the tectonic evolution of the northern Xinjiang, Northwest China (in Chinese), *Geosci. Xinjiang*, *1*, 47–68.

Xiao, X. C., Y. Q. Tang, Y. M. Feng, B. Q. Zhu, J. Y. Li, and M. Zhao (Eds.) (1992), *Tectonics in Northern Xinjiang and Its Neighbouring Areas*, pp. 104–121, Geol. Publ., Beijing.

Xu, B., P. Jian, H. F. Zheng, H. B. Zou, L. F. Zhang, and D. Y. Liu (2005), U-Pb zircon geochronology and creochemistry of Neoproterozoic volcanic rocks in the Tarim Block of northwest China: Implications for the breakup of Rodinia supercontinent and Neoproterozoic glaciations, *Precambrian Res.*, *136*, 107–123.

Yuan, C., W. J. Xiao, H. L. Chen, J. L. Li, and M. Sun (2006), Zhaheba potassic basalt, eastern Junggar (NW China): Geochemical characteristics and tectonic implications (in Chinese), *Acta Geol. Sin.*, *80*, 254–263.

Yuan, C., M. Sun, W. J. Xiao, X. H. Li, H. L. Chen, S. F. Lin, X. P. Xia, and X. P. Long (2007), Accretionary orogenesis of the Chinese Altai: Insights from Paleozoic granitoids, *Chem. Geol.*, *242*, 22–39.

Yuan, X. C. (1995), Remark on structure of China continental basement, *Acta Geophys. Sin.*, *38*(4), 448–459.

Zhai, M. G., and W. J. Liu (2003), Palaeoproterozoic tectonic history of the North China craton: A review, *Precambrian Res.*, *122*, 183–199.

Zhai, M. G., J. A. Shao, J. Hao, and P. Peng (2003), Geological signature and possible position of the North China Block in the supercontinent Rodinia, *Gondwana Res.*, *6*, 171–183.

Zhang, C., M. Zhai, M. B. Allen, A. D. Saunders, G. Wang, and X. Huang (1993), Implications of Paleozoic ophiolites from West Junggar, NW China for the tectonic of central Asia, *J. Geol. Soc.*, *150*, 551–561.

Zhang, C. L., Z. X. Li, X. H. Li, H. M. Ye, A. G. Wang, and K. Y. Guo (2006), Neoproterozoic bimodal intrusive complex in the southwestern Tarim Block,

northwest China: Age, geochemistry, and implications for the rifting of Rodinia, *Int. Geol. Rev.*, *48*, 112–128.
Zhang, J. H., J. B. Wang, and R. F. Ding (2000), Characteristics and U-Pb ages of zircons in metavolcanics from the Kangbutiebao Formation in the Altai Orogen, Xinjiang, *Reg. Geol. China*, *19*, 281–287.
Zhang, Z. Q., Q. H. Shen, Y. S. Geng, S. H. Tang, and J. H. Wang (1996), Geochemistry and ages of Archean metamorphic rocks in northwestern Hebei Province, China, and formation time of the paleocrust in the region, *Acta Pet. Sin.*, *12*, 315–328.
Zhao, G. C., P. A. Cawood, S. A. Wilde, M. Sun, and L. Lu (2000), Metamorphism of basement rocks in the Central Zone of the North China craton: Implications for Palaeoproterozoic tectonic evolution, *Precambrian Res.*, *103*, 55–88.
Zhao, G. C., M. Sun, S. A. Wilde, and S. Z. Li (2005), Late Archean to Paleoproterozoic evolution of the North China Craton: Key issues revisited, *Precambrian Res.*, *136*, 177–202.
Zheng, C. Q., X. C. Xu, M. Enami, and T. Kato (2005), Monazite ages and geological implication of andalusite-sillimanite type metamorphic belt in Aletai, Xinjiang (in Chinese), *Global Geol.*, *24*(3), 236–242.
Zhou, Y. Q. (1994), Discussion on the basement property of Junggar basin, *Geosci. Xinjiang*, *5*, 19–27.
Zhuang, Y. X. (Ed.) (1994a), *Tectonothermal Evolution in Space and Time and Orogenic Process of Aletai, China*, pp. 70–106, Jilin Sci. and Technol. Press, Changchun, China.
Zhuang, Y. X. (1994b), The pressure-temperature-space-time (PTSt) evolution of metamorphism and development mechanism of the thermal-structural-gneiss domes in the Chinese Altaids, *Acta. Geol. Sin.*, *68*, 35–47.
Zorin, Y. A., V. G. Belichenko, E. K. Turutanov, V. M. Kozhevnikov, S. V. Ruzhentsev, A. B. Dergunov, and I. B. Filippova (1993), The South Siberia-Central Mongolia transect, *Tectonophysics*, *225*, 361–378.

K. Cai, X. Long, and C. Yuan, Key Laboratory of Isotope Geochronology and Geochemistry, Guangzhou Institute of Geochemistry, Chinese Academy of Sciences, Guangzhou 510640, China.

S. Lin, Department of Earth Sciences, University of Waterloo, Waterloo, ON, Canada N2L 3G1.

M. Sun (corresponding author) and X. Xia, Department of Earth Sciences, University of Hong Kong, Pokfulam Road, Hong Kong, China. (minsun@hkucc.hku.hk)

F. Wu and W. Xiao, State Key Laboratory of Lithospheric Evolution, Institute of Geology and Geophysics, Chinese Academy of Sciences, Beijing 100029, China.